Homogenization for Sea Ice and the Climate System

Kenneth M. Golden
Department of Mathematics
University of Utah

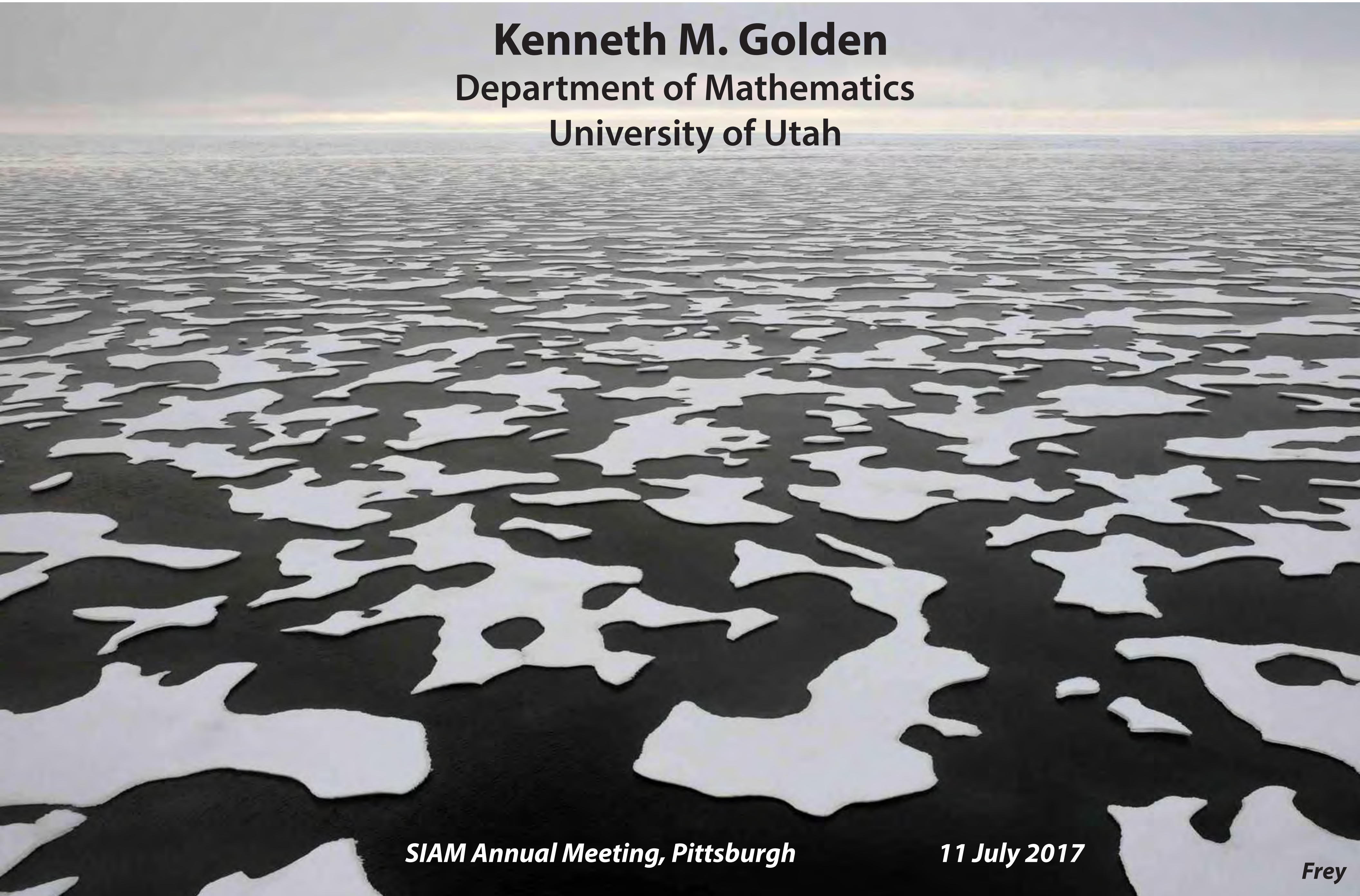

Frey

SIAM Annual Meeting, Pittsburgh ***11 July 2017***

ANTARCTICA

southern cryosphere

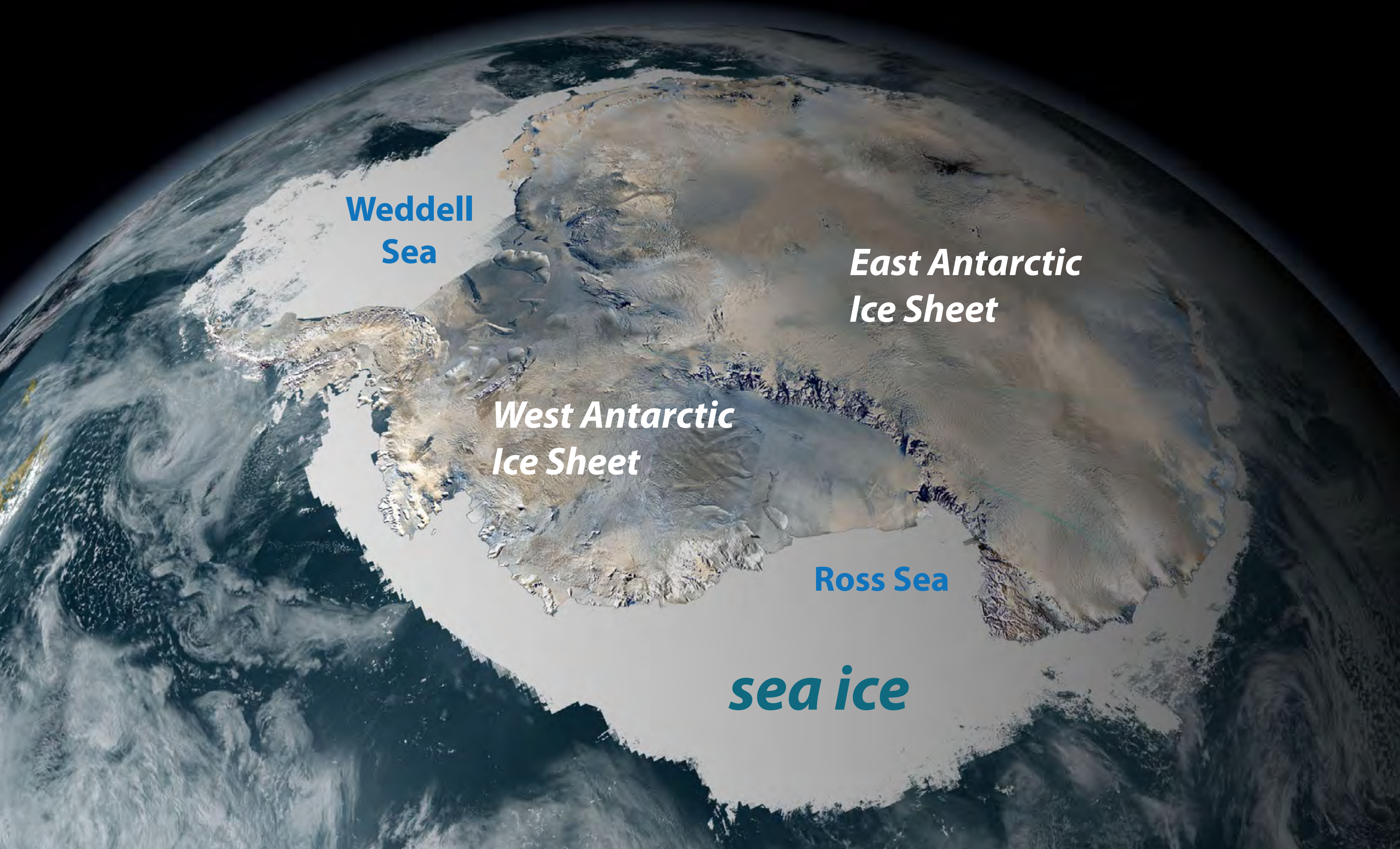


SEA ICE covers 7 - 10% of earth's ocean surface
• boundary between ocean and atmosphere
• mediates exchange of heat, gases, momentum
• global ocean circulation
• indicator and agent of climate change

polar ice caps critical to global climate in reflecting incoming solar radiation

white snow and ice reflect

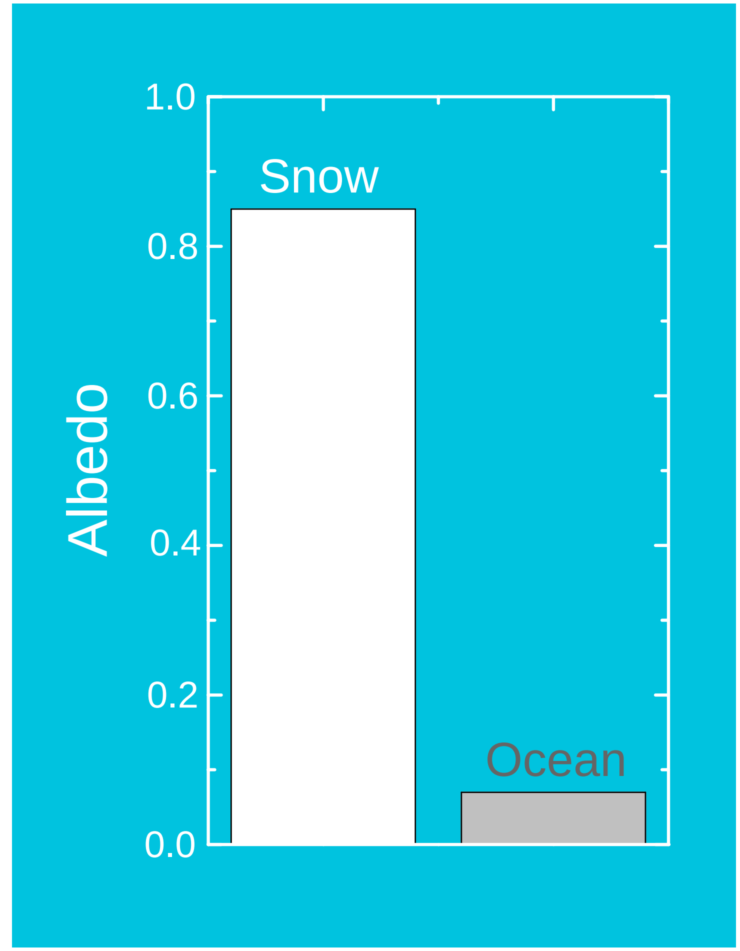

dark water and land absorb

$$\textbf{\textit{albedo}}\ \alpha = \frac{\text{reflected sunlight}}{\text{incident sunlight}}$$

the summer Arctic sea ice pack is melting

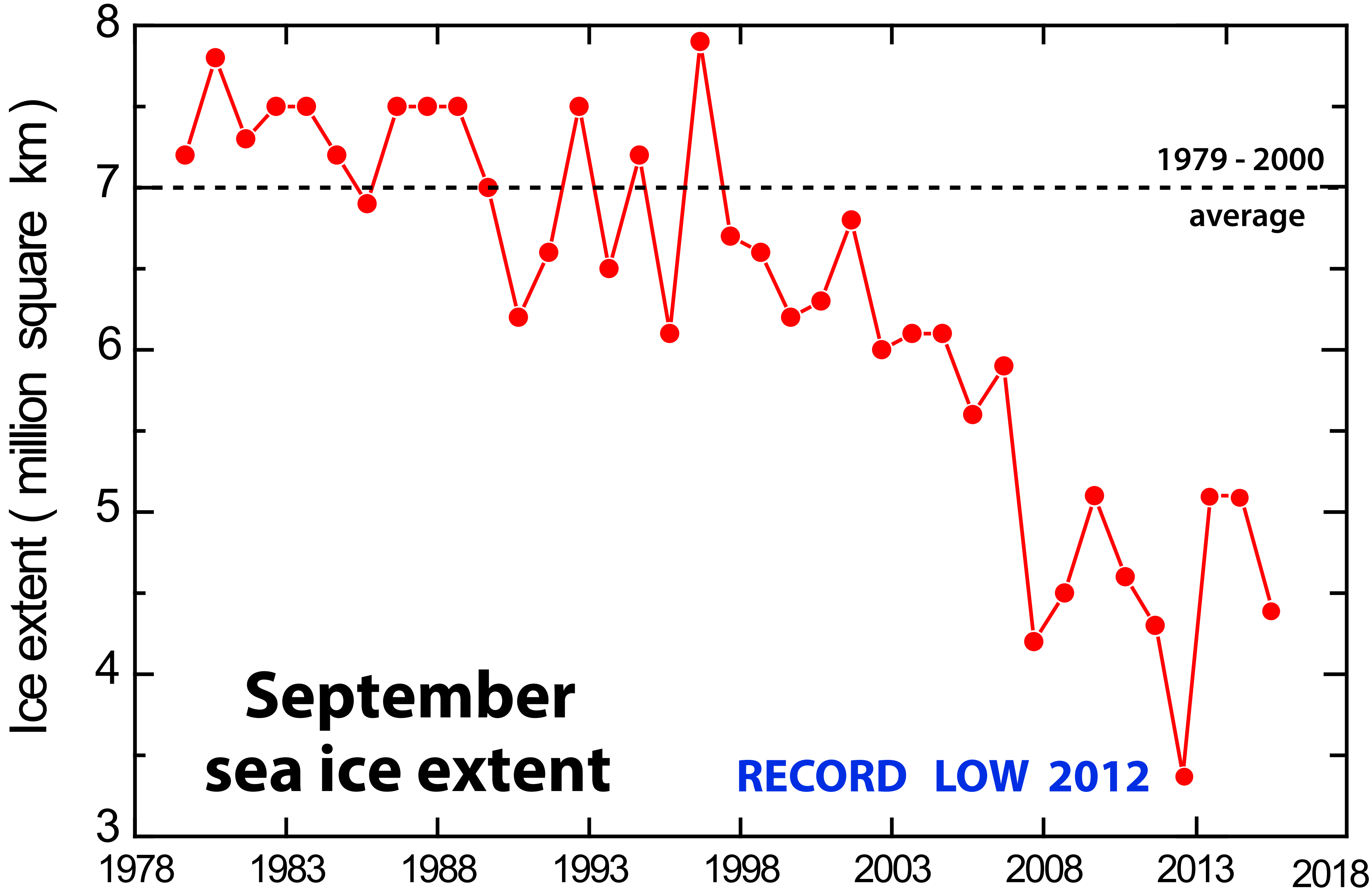

National Snow and Ice Data Center

Change in Arctic Sea Ice Extent

September 1980 -- 7.8 million square kilometers
September 2012 -- 3.4 million square kilometers

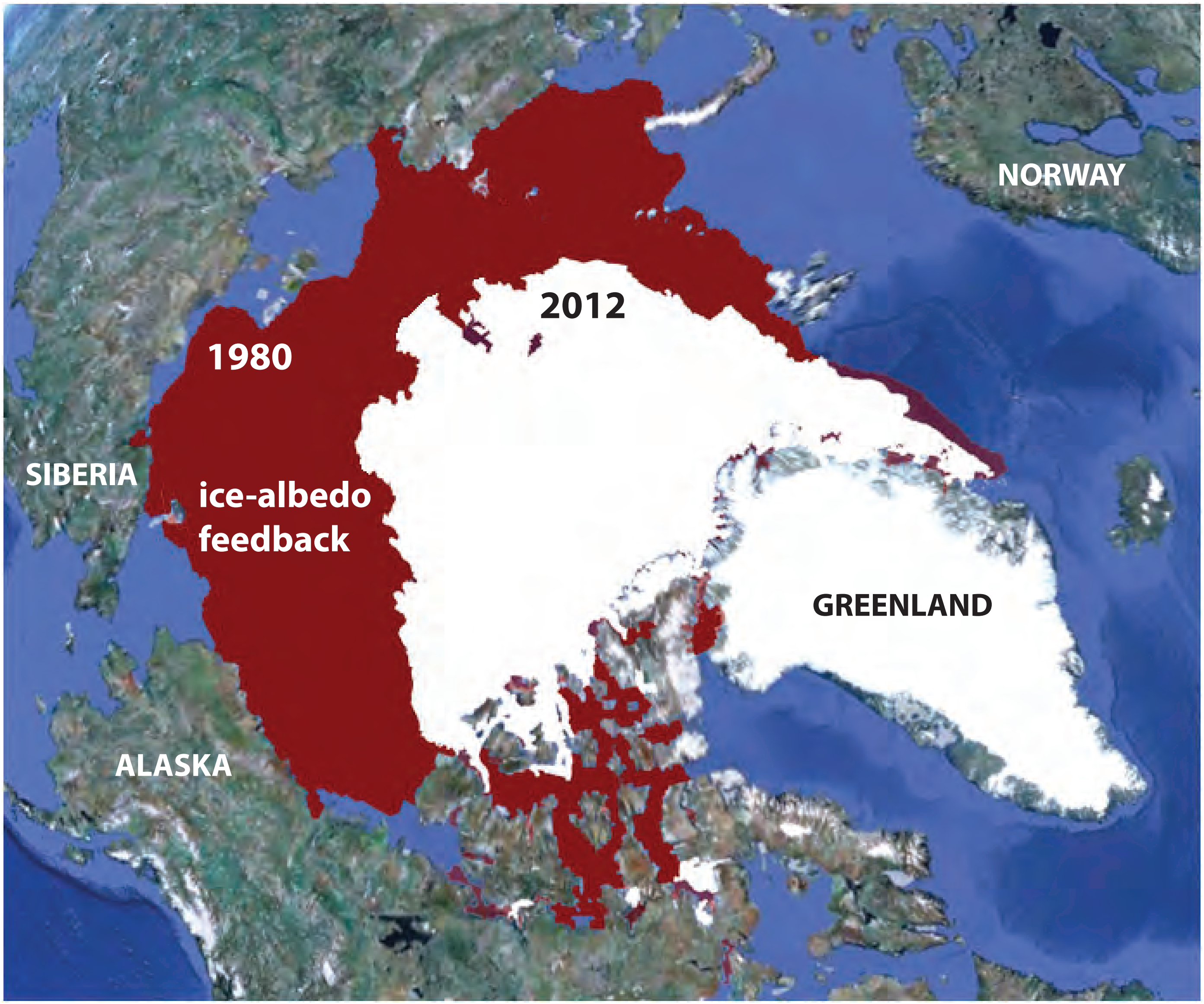

Perovich

Arctic sea ice decline - faster than predicted by climate models

Stroeve et al., GRL, 2007

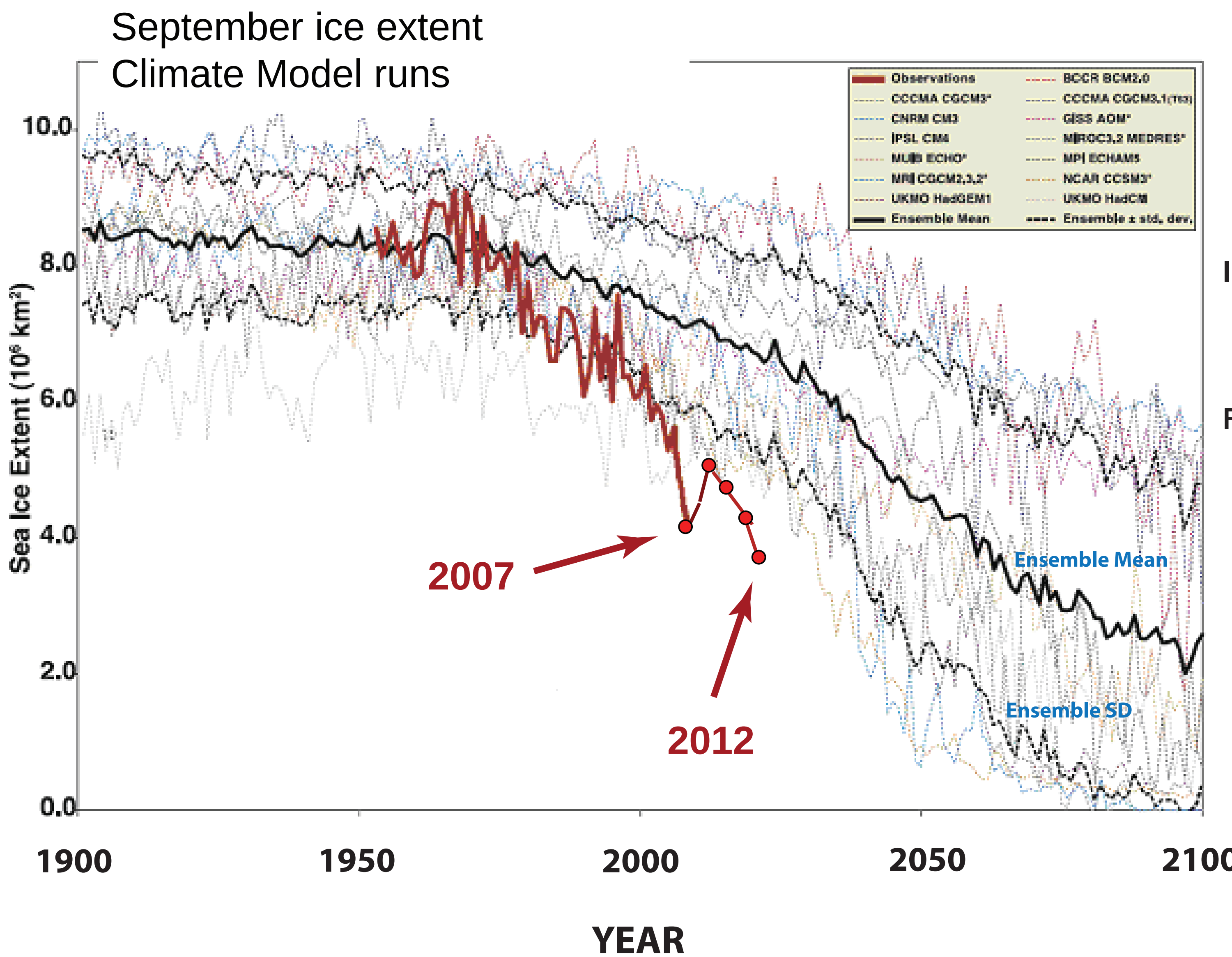

IPCC AR4 Models

Intergovernmental Panel on Climate Change (IPCC)

Fourth Assessment AR4, 2007

challenge

represent sea ice more rigorously in climate models

account for key processes

such as melt pond evolution

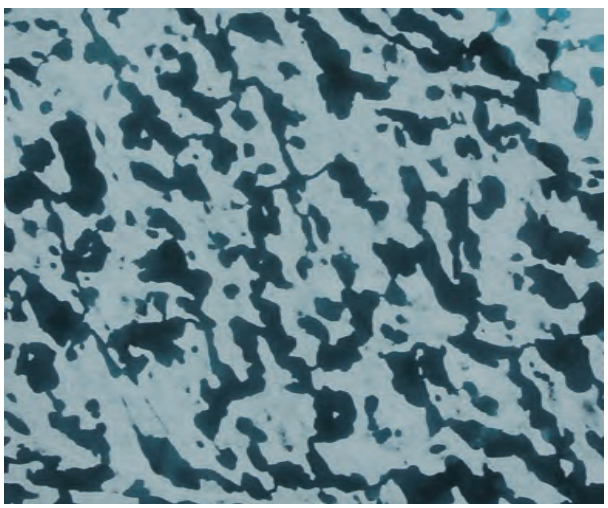

Impact of melt ponds on Arctic sea ice simulations from 1990 to 2007

Flocco, Schroeder, Feltham, Hunke, *JGR Oceans* 2012

For simulations with ponds September ice volume is nearly 40% lower.

... and other sub-grid scale structures and processes

linkage of scales

sea ice is a multiscale composite

displaying structure over 10 orders of magnitude

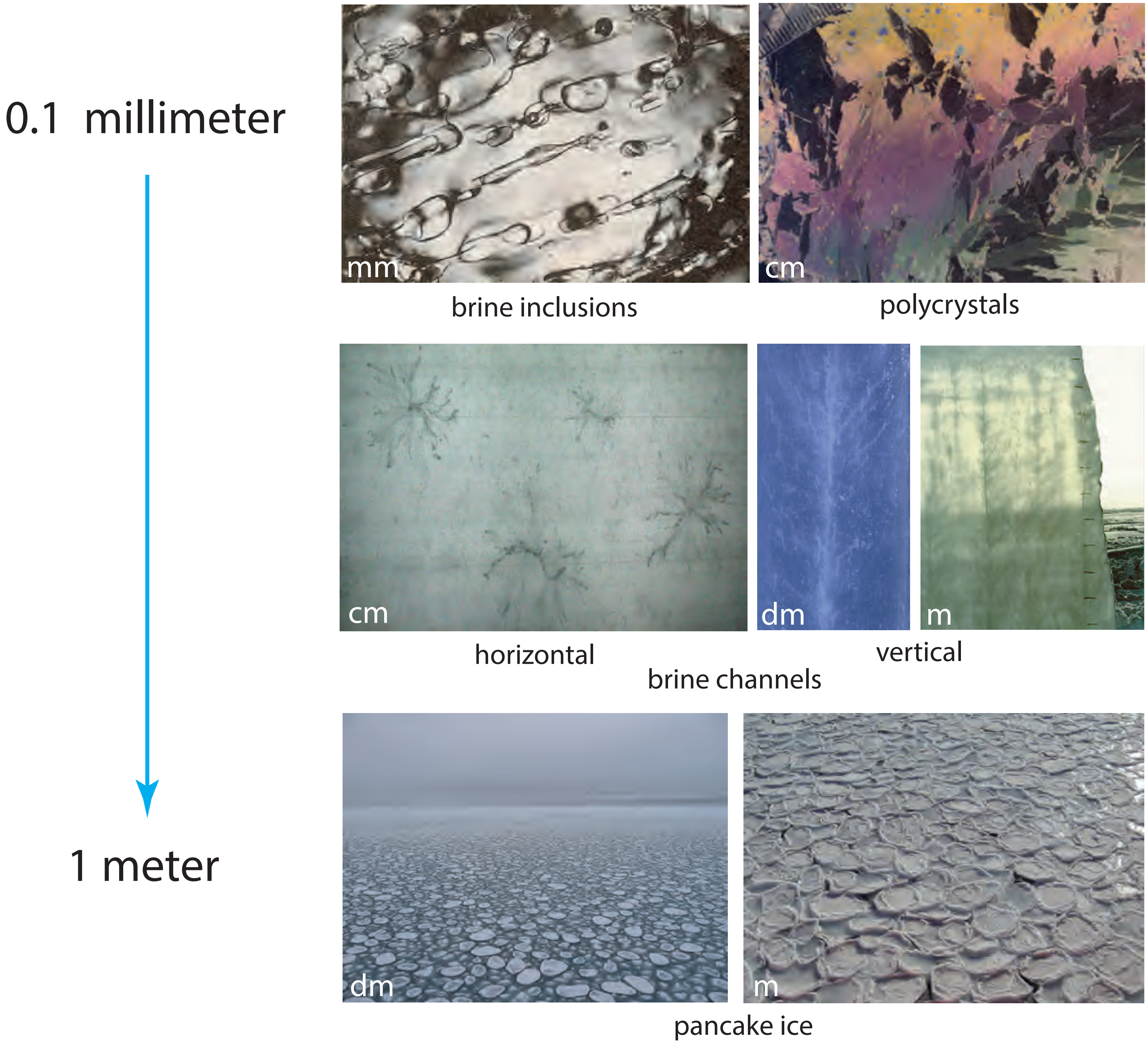

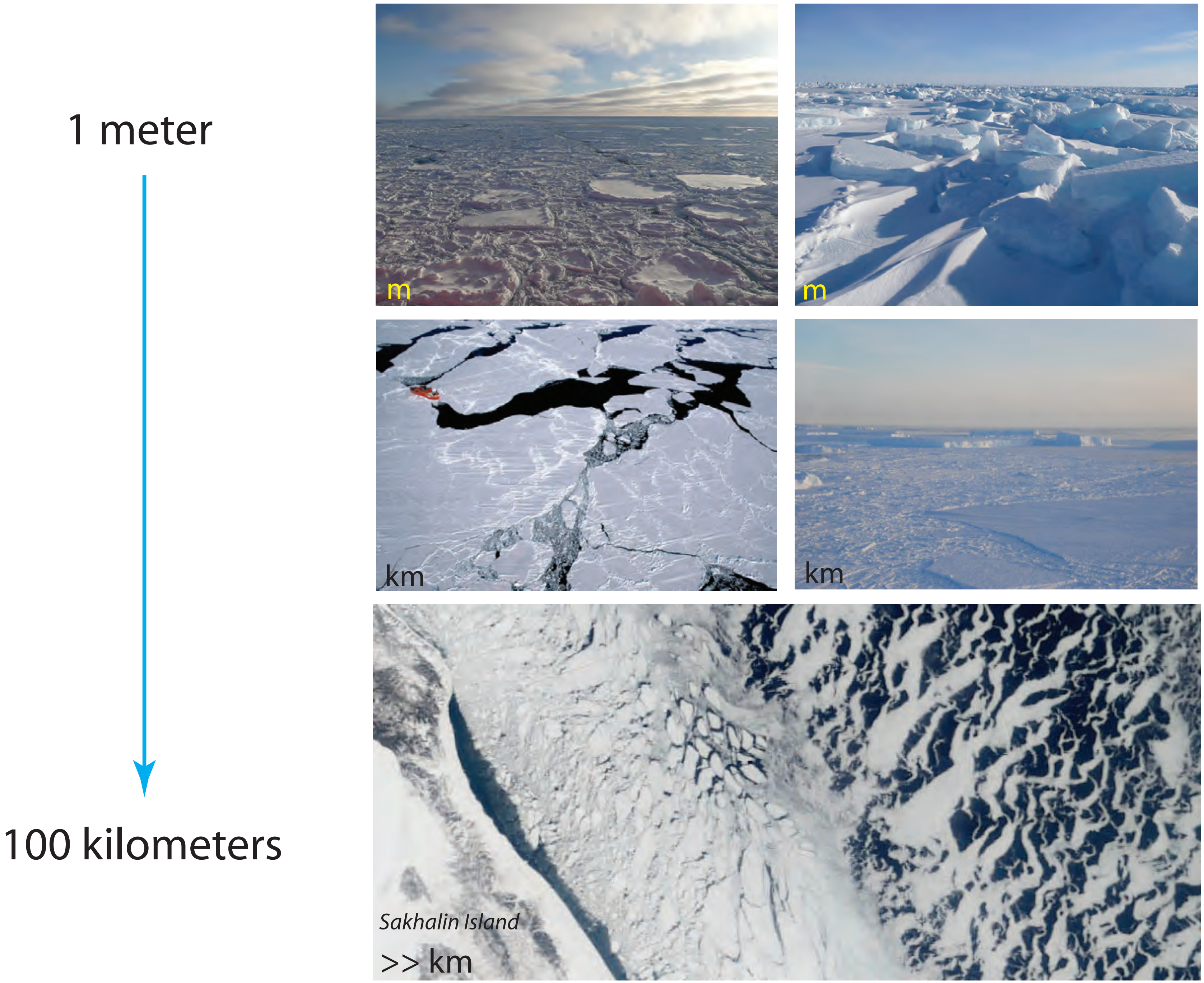
1 meter
100 kilometers
m
m
km
km
Sakhalin Island
>> km

What is this talk about?

Using the mathematics of composite materials and statistical physics to study sea ice structures and processes ... to improve projections of climate change.

HOMOGENIZATION

1. Climate modeling and the polar ice packs

systems of partial differential equations

2. Sea ice microphysics and porous media

fluid flow, diffusion processes, percolation theory

3. EM monitoring of sea ice

integral representations, spectral measures, random matrix theory

4. Advection diffusion; polycrystals; waves in the MIZ

integral representations, bounds

5. Evolution of Arctic melt ponds, fractal geometry

continuum percolation, network and Ising models

critical behavior ***cross - pollination***

Global Climate Models

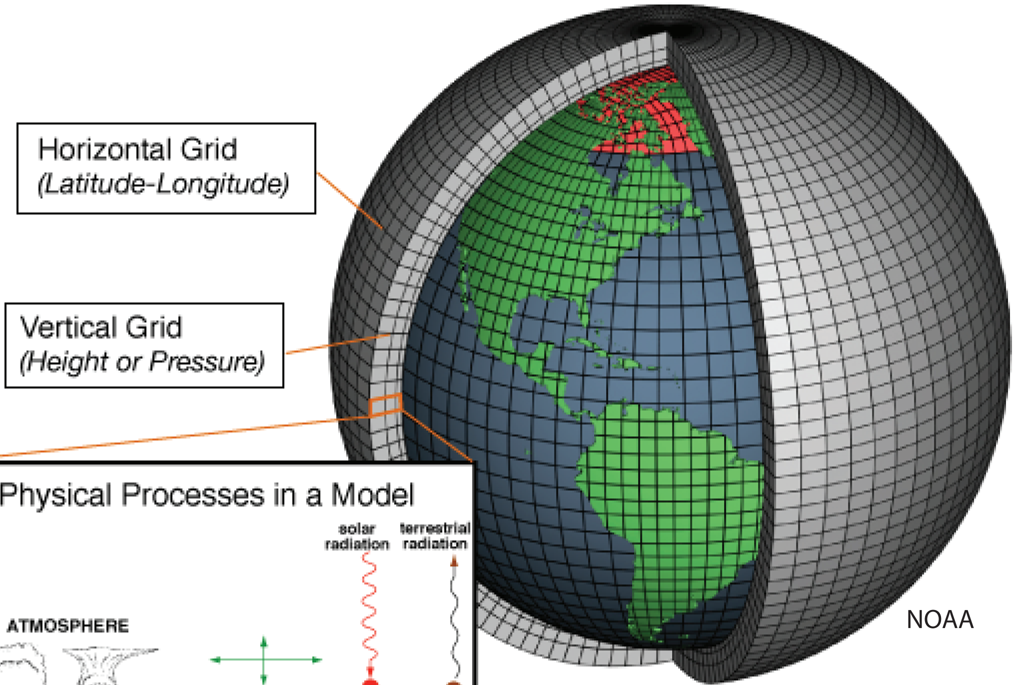

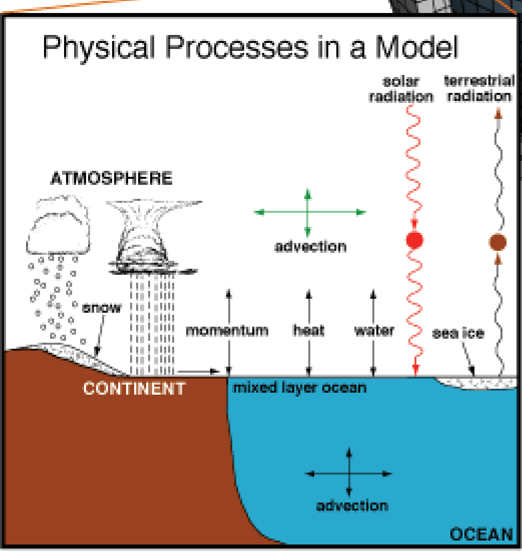

NOAA

Climate models are systems of partial differential equations (PDE) derived from the basic laws of physics, chemistry, and fluid motion.

They describe the state of the ocean, ice, atmosphere, land, and their interactions.

The equations are solved on 3-dimensional grids of the air-ice-ocean-land system (with horizontal grid size ~ 50 km), using very powerful computers.

key challenge :

incorporating sub - grid scale processes

linkage of scales

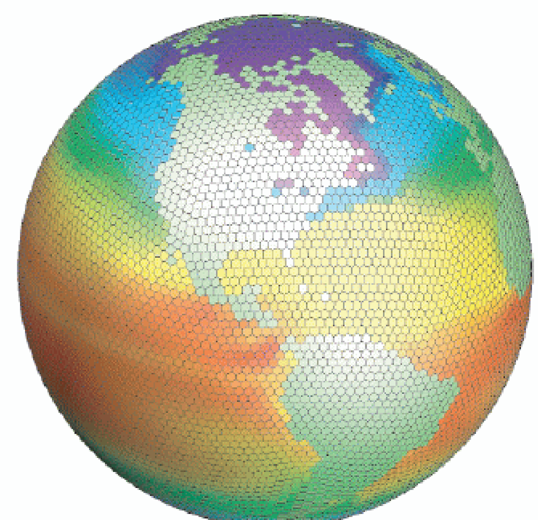

Randall *et al.*, 2002

sea ice components of GCM's

What are the key ingredients -- or ***governing equations*** that need to be solved on grids using powerful computers?

1. Ice thickness distribution $g(x, y, h, t)$ evolution equation

dynamics + ***thermodynamics***

(Thorndike *et al.* 1975)

$$\frac{Dg}{Dt} = -g\nabla \cdot \mathbf{u} + \Psi(g) - \frac{\partial}{\partial h}(\tau g) + \mathcal{L}$$

nonlinear PDE with ice velocity field

ice growth ice melting

mechanical redistribution - ridging and opening

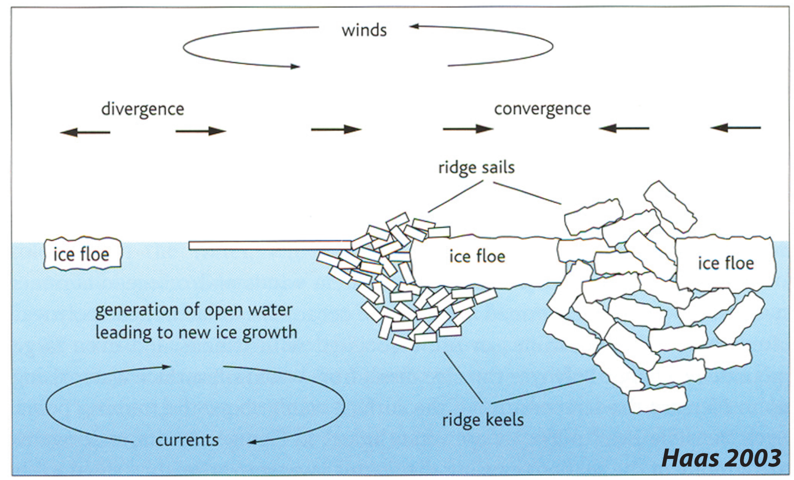

2. Conservation of momentum, stress *vs.* strain relation (Hibler 1979)

$$m\frac{D\mathbf{u}}{Dt} = -mf\mathbf{k} \times \mathbf{u} + \boldsymbol{\tau}_a + \boldsymbol{\tau}_o - mg\nabla H + \mathbf{F}_{int}$$

F = ma **for sea ice** ***dynamics***

3. Heat equation of sea ice and snow

(Maykut and Untersteiner 1971)

$$\frac{\partial T}{\partial t} + \mathbf{u}_{br} \cdot \nabla T = \nabla \cdot k(T)\,\nabla T$$

thermodynamics

+ ***balance of radiative and thermal fluxes on interfaces***

sea ice microphysics

fluid transport

fluid flow through the porous microstructure of sea ice governs key processes in polar climate and ecosystems

evolution of Arctic melt ponds and sea ice albedo

nutrient flux for algal communities

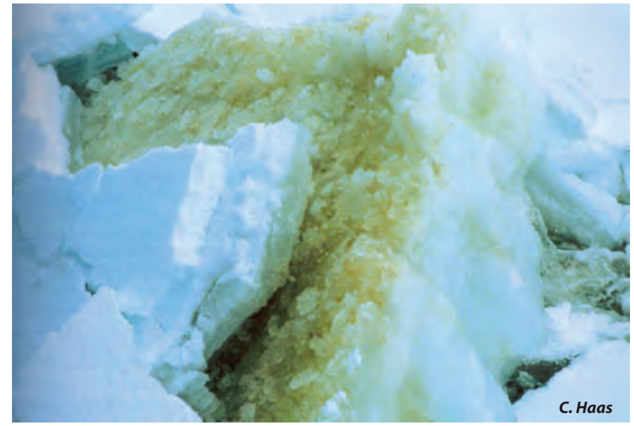

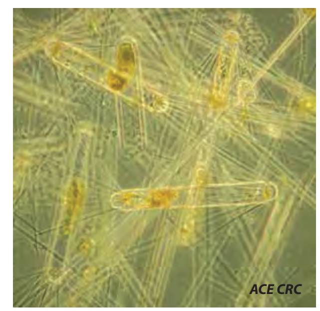

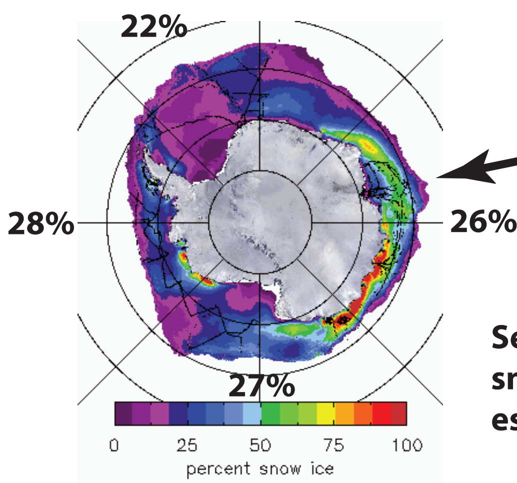

T. Maksym and T. Markus, 2008

September snow-ice estimates

Antarctic surface flooding and snow-ice formation

- *evolution of salinity profiles*
- *ocean-ice-air exchanges of heat, CO_2*

sea ice ecosystem

sea ice algae
support life in the polar oceans

fluid permeability *k* of a porous medium

porous concrete

how much water gets through the sample per unit time?

HOMOGENIZATION

mathematics for analyzing effective behavior of heterogeneous systems

HOMOGENIZE as $\epsilon \to 0$

Stokes equations for fluid velocity $\mathbf{v}^\epsilon$, pressure p^ϵ, force $\mathbf{f}$:

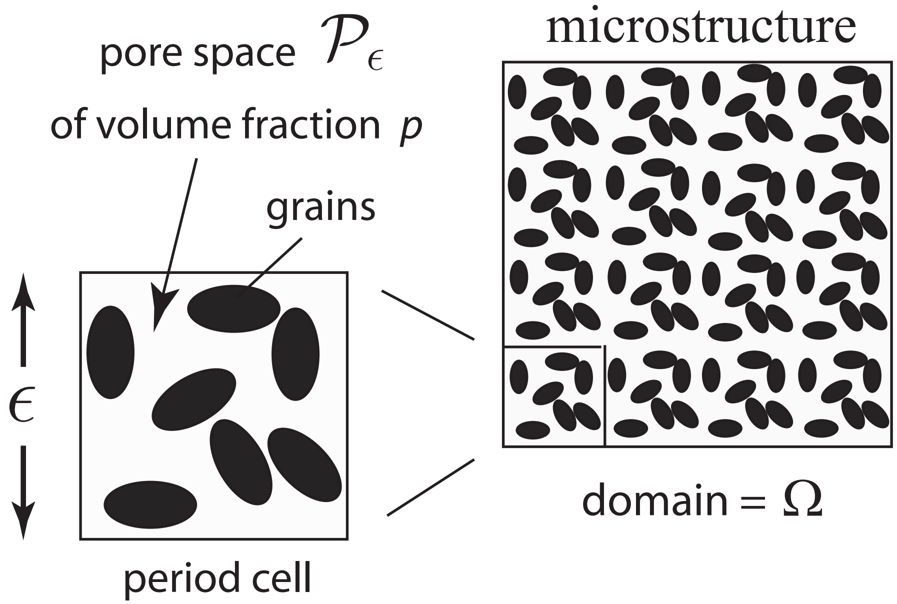

$$\nabla p^\epsilon - \epsilon^2 \eta \Delta \mathbf{v}^\epsilon = \mathbf{f}, \qquad x \in \mathcal{P}_\epsilon$$

$$\nabla \cdot \mathbf{v}^\epsilon = 0, \qquad x \in \mathcal{P}_\epsilon$$

$$\mathbf{v}^\epsilon = 0, \qquad x \in \partial\mathcal{P}_\epsilon$$

η = fluid viscosity

via two-scale expansion

MACROSCOPIC EQUATIONS $\mathbf{v}^\epsilon \to \mathbf{v}$, $p^\epsilon \to p$ as $\epsilon \to 0$

Darcy's law (f = 0)

$$\mathbf{v} = -\frac{1}{\eta}\,\mathbf{k}\,\nabla p, \qquad x \in \Omega$$

$$\nabla \cdot \mathbf{v} = 0, \qquad x \in \Omega$$

$\mathbf{k}(x)$ = effective fluid permeability tensor

[Keller '80, Tartar '80, Sanchez-Palencia '80, J. L. Lions '81, Allaire '89, '91,'97]

Darcy's Law for slow viscous flow in a porous medium

averaged fluid velocity

pressure gradient

$$\mathrm{v} = -\frac{\mathbf{k}}{\eta}\nabla p$$

viscosity

$\mathbf{k}$ = fluid permeability tensor

PIPE BOUNDS on vertical fluid permeability k

Golden, Heaton, Eicken, Lytle, Mech. Materials 2006
Golden, Eicken, Heaton, Miner, Pringle, Zhu, Geophys. Res. Lett. 2007

vertical pipes

with appropriate radii

maximize k

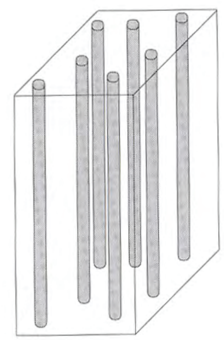

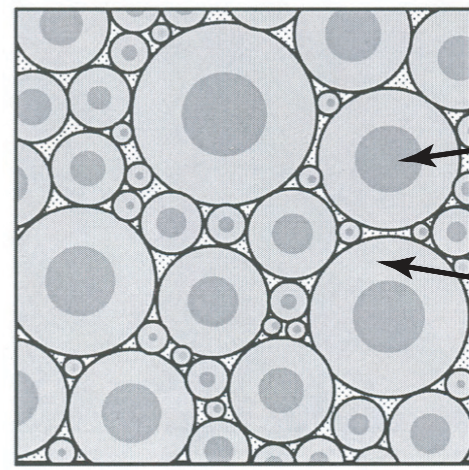

optimal coated cylinder geometry

fluid analog of arithmetic mean upper bound for effective conductivity of composites (Wiener 1912)

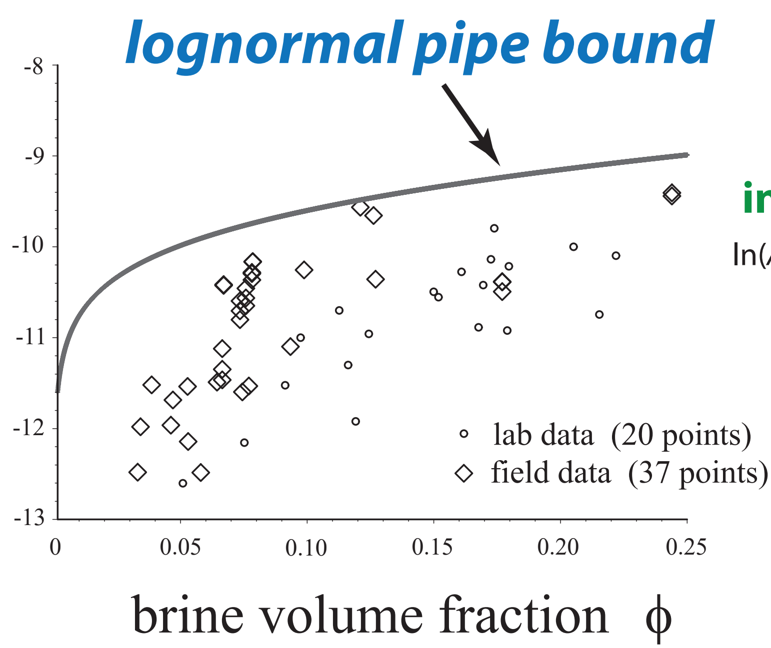

Golden et al., Geophys. Res. Lett. 2007

$$k \leq \frac{\phi \langle R^4 \rangle}{8 \langle R^2 \rangle} = \frac{\phi}{8} \langle R^2 \rangle e^{\sigma^2}$$

inclusion cross sectional areas A lognormally distributed

ln(A) normally distributed, mean μ (increases with T) variance σ^2 (Gow and Perovich 96)

get bounds through variational analyis of ***trapping constant*** γ for diffusion process in pore space with absorbing BC

Torquato and Pham, *PRL* 2004

$$\mathbf{k} \leq \gamma^{-1} \mathbf{I}$$

for any ergodic porous medium (Torquato 2002, 2004)

Critical behavior of fluid transport in sea ice

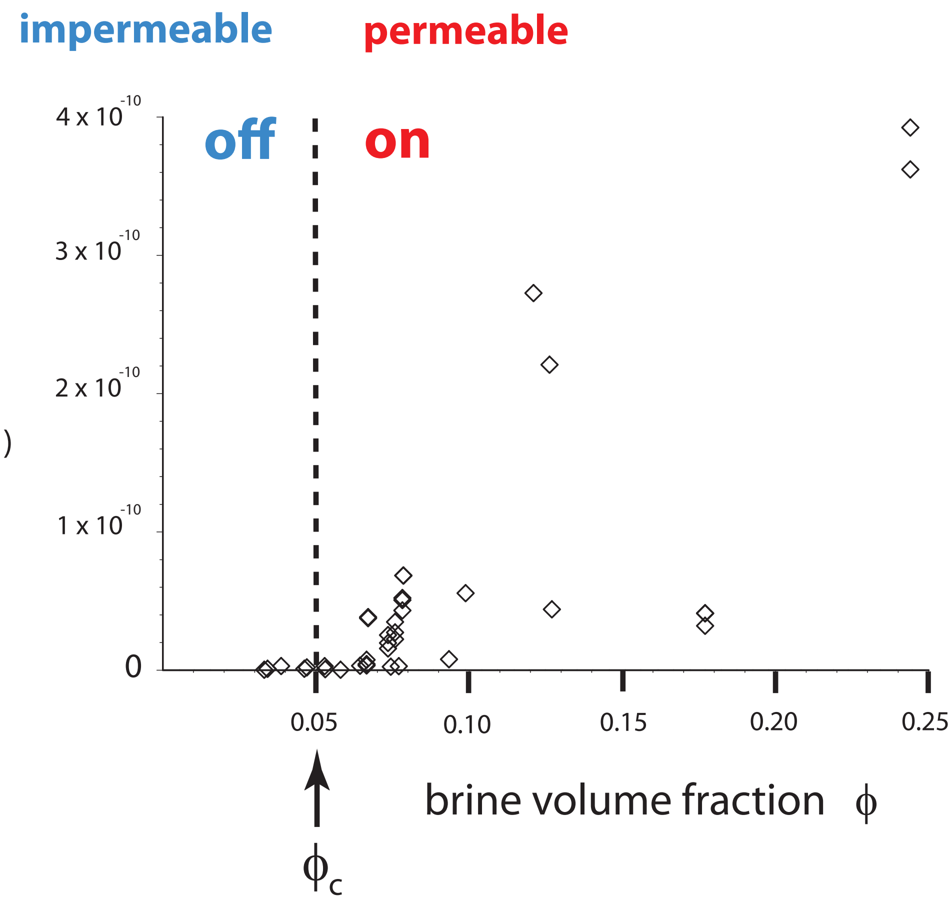

Arctic field data

vertical fluid permeability k (m ^{2})

on - off switch for fluid flow

critical brine volume fraction $\phi_c \approx 5\%$ ⟷ $T_c \approx -5^\circ C, \; S \approx 5$ ppt

RULE OF FIVES

Golden, Ackley, Lytle *Science* 1998

Golden, Eicken, Heaton, Miner, Pringle, Zhu, *Geophys. Res. Lett.* 2007

Pringle, Miner, Eicken, Golden *J. Geophys. Res.* 2009

sea ice algal communities

D. Thomas 2004

nutrient replenishment controlled by ice permeability

biological activity turns on or off according to *rule of fives*

critical behavior of microbial activity

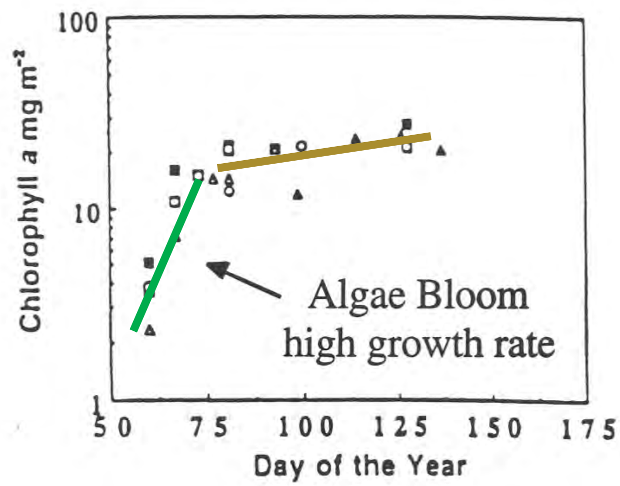

Convection-fueled algae bloom
Ice Station Weddell

Golden, Ackley, Lytle ***Science 1998***

Fritsen, Lytle, Ackley, Sullivan ***Science 1994***

Why is the rule of fives true?

percolation theory

probabilistic theory of connectedness

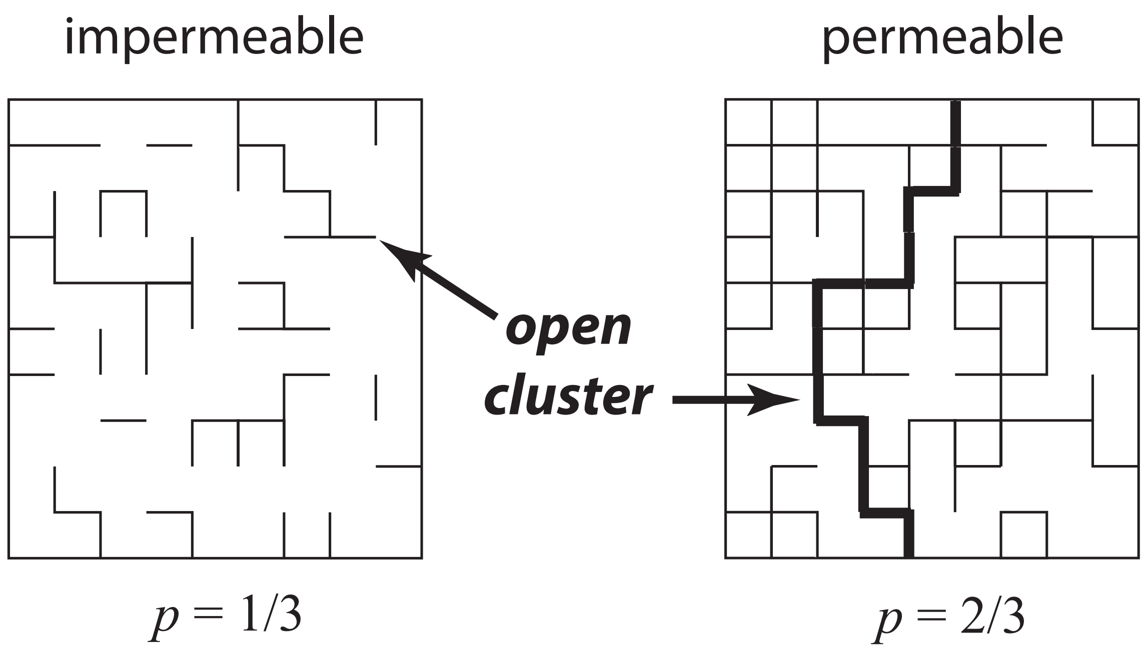

bond → **open** *with probability p*
closed *with probability 1-p*

percolation threshold

$$p_c = 1/2 \quad \text{for} \quad d = 2$$

smallest *p* for which there is an infinite open cluster

order parameters in percolation theory

geometry

correlation length

characteristic scale
of connectedness

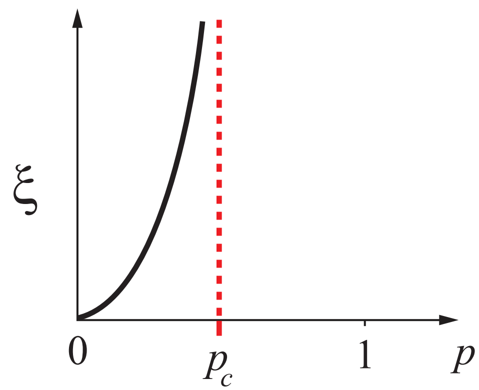

$$\xi(p) \sim |p - p_c|^{-\nu}$$

$$p \to p_c$$

infinite cluster density

probability the origin
belongs to infinte cluster

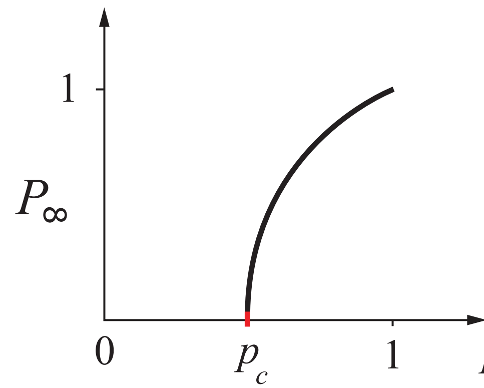

$$P_\infty(p) \sim (p - p_c)^\beta$$

$$p \to p_c^+$$

transport

effective conductivity or fluid permeability

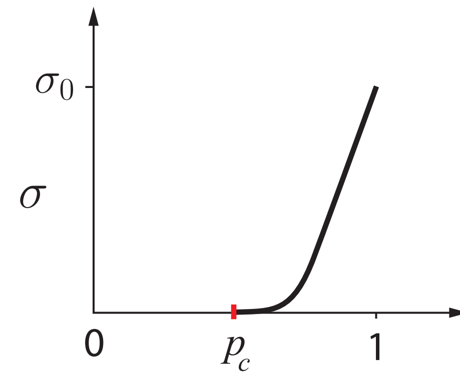

$$\sigma(p) \sim \sigma_0 \, (p - p_c)^t$$

$$p \to p_c^+$$

UNIVERSAL critical exponents for lattices -- depend only on dimension

$1 \le t \le 2$ (for idealized model), Golden, *Phys. Rev. Lett.* 1990 ; *Comm. Math. Phys.* 1992

non-universal behavior in continuum

Continuum percolation model for ***stealthy*** materials applied to sea ice microstructure explains **Rule of Fives** and Antarctic data on ice production and algal growth

$\phi_c \approx 5\,\%$ Golden, Ackley, Lytle, *Science*, 1998

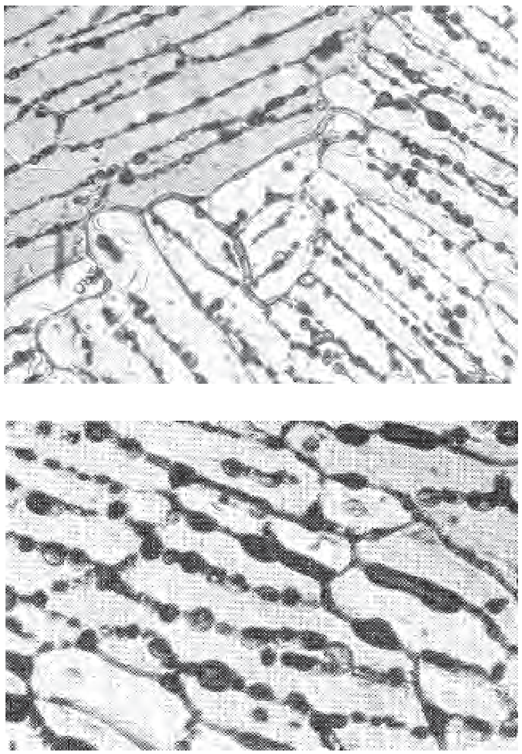

sea ice

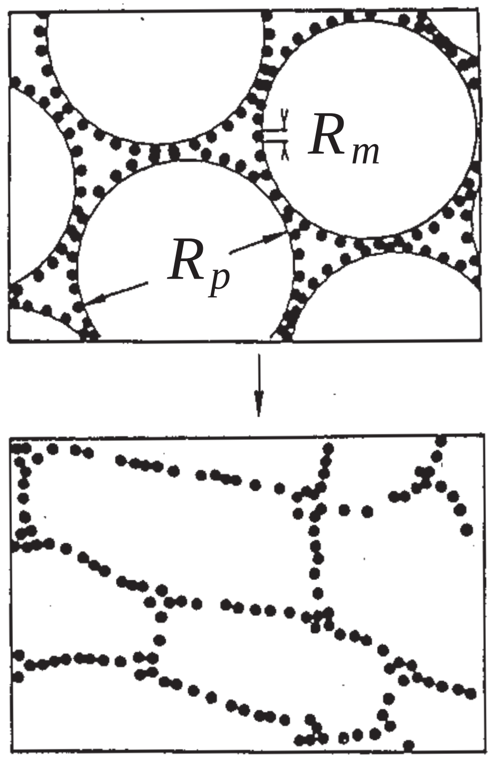

compressed powder

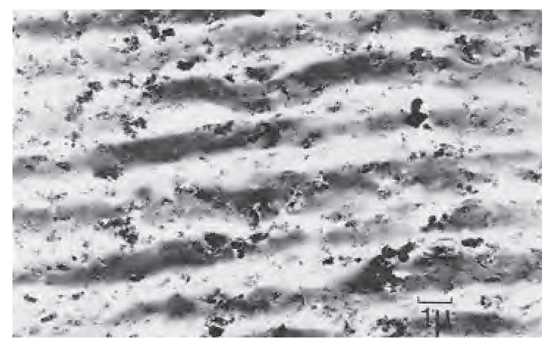

radar absorbing composite

sea ice is radar absorbing

Thermal evolution of permeability and microstructure in sea ice ***Golden, Eicken, Heaton, Miner, Pringle, Zhu***

micro-scale

controls

macro-scale processes

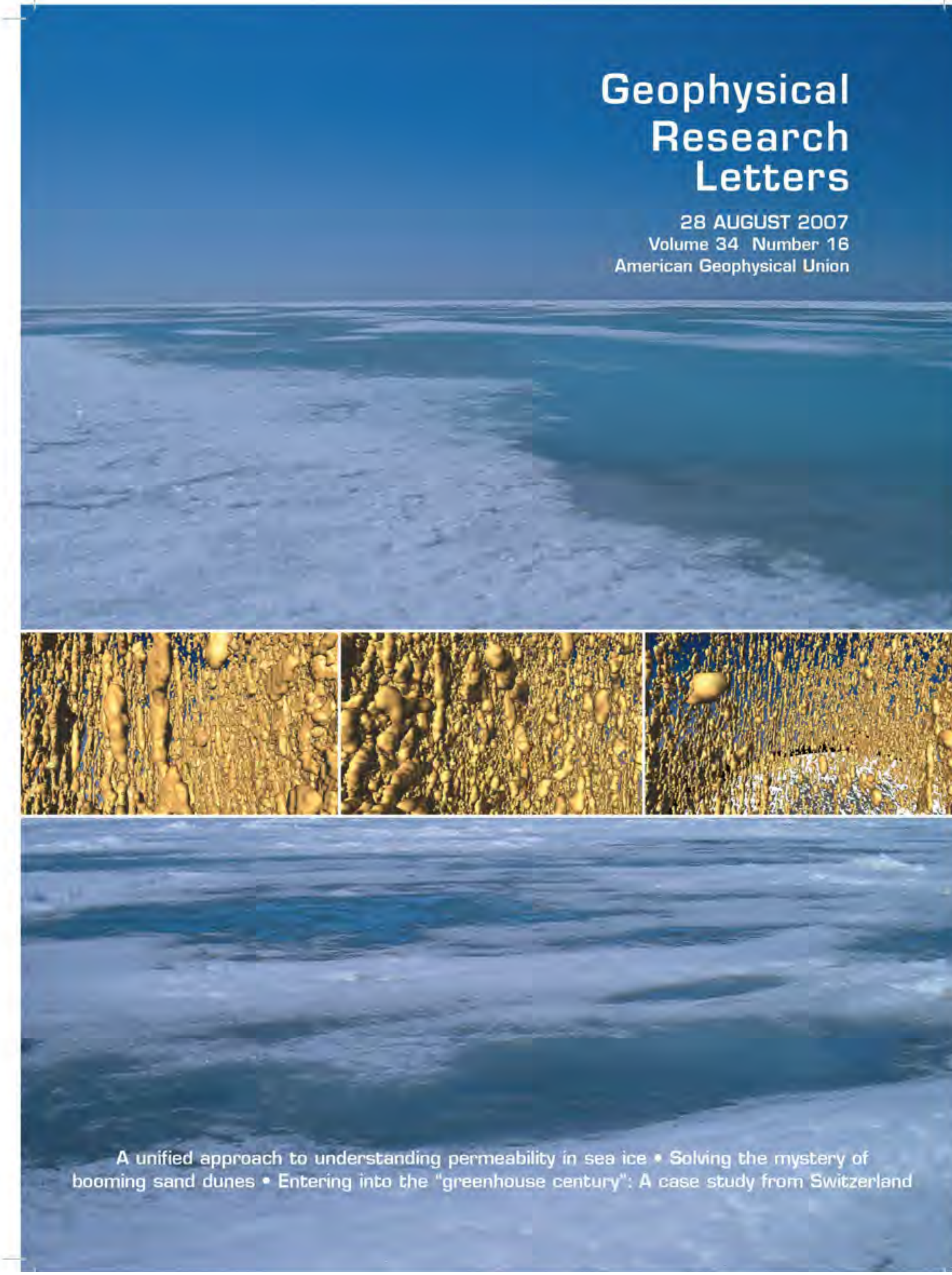

rigorous bounds
percolation theory
hierarchical model
network model

field data

X-ray tomography for brine inclusions

unprecedented look at thermal evolution of brine phase and its connectivity

brine connectivity (over cm scale)

8 x 8 x 2 mm

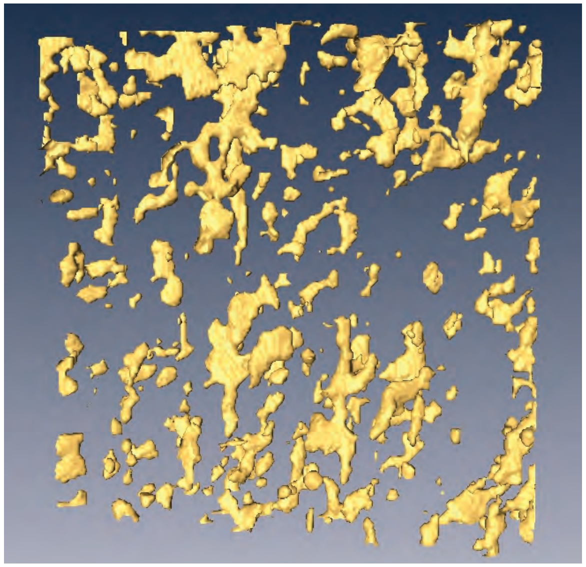

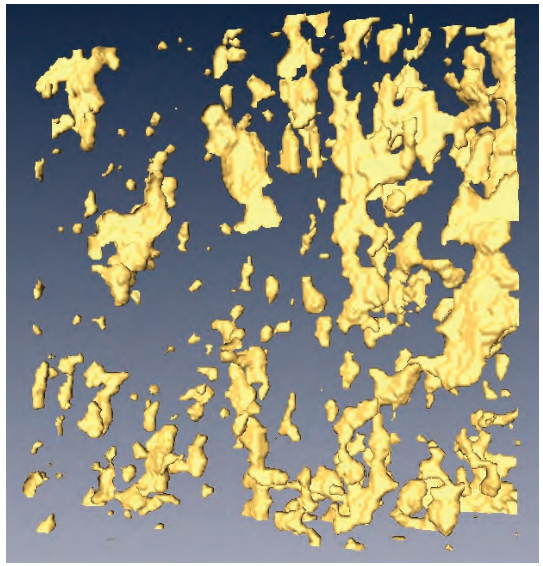

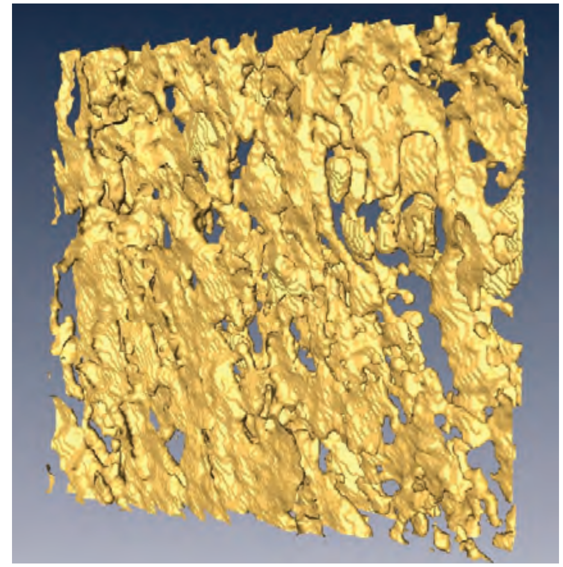

-15 °C, $\phi = 0.033$ -6 °C, $\phi = 0.075$ -3 °C, $\phi = 0.143$

X-ray tomography confirms percolation threshold

3-D images
pores and throats → 3-D graph
nodes and edges

analyze graph connectivity as function of temperature and sample size

- ***use finite size scaling techniques to confirm rule of fives***
- ***order parameter data from a natural material***

Pringle, Miner, Eicken, Golden, J. Geophys. Res. 2009

lattice and continuum percolation theories yield:

$$k(\phi) = k_0 (\phi - 0.05)^2$$

critical exponent t

$$k_0 = 3 \times 10^{-8} \text{ m}^2$$

- exponent is UNIVERSAL lattice value $t \approx 2.0$
- sedimentary rocks like sandstones also exhibit universality
- critical path analysis -- developed for electronic hopping conduction -- yields scaling factor k_0

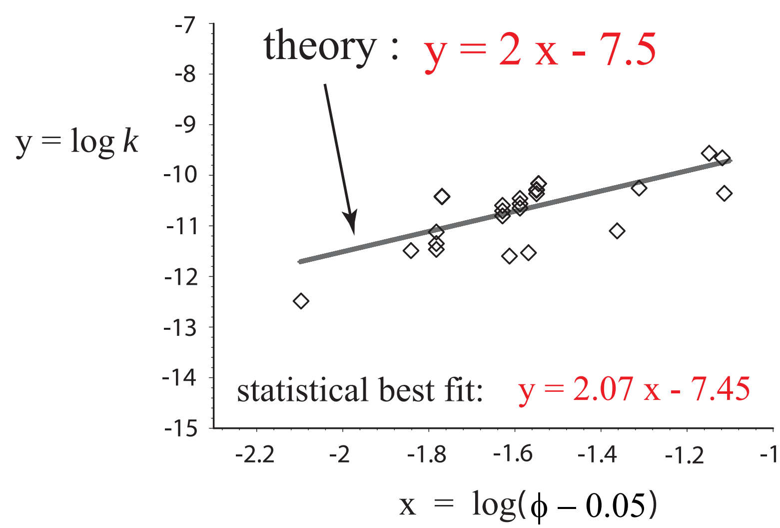

Sea ice algae secrete extracellular polymeric substances (EPS) affecting evolution of brine microstructure.

How does EPS affect fluid transport?

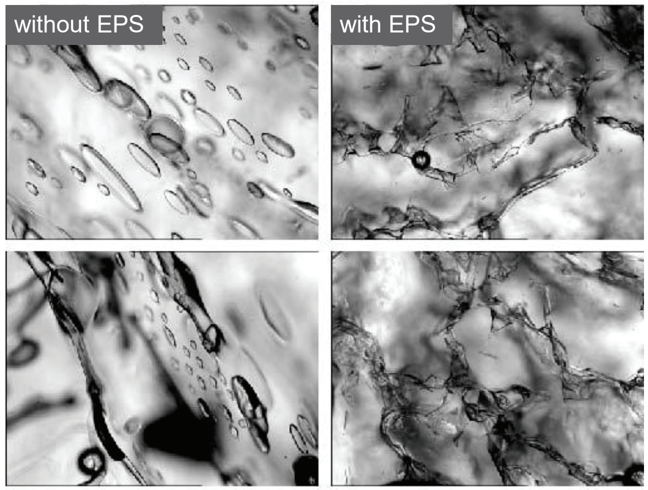

Krembs, Eicken, Deming, PNAS 2011

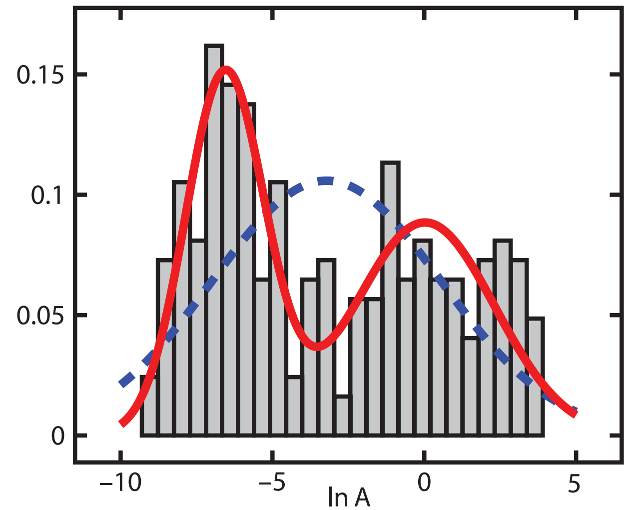

- **Bimodal** lognormal distribution for brine inclusions
- Develop random pipe network model with bimodal distribution; Use numerical methods that can handle larger variances in sizes.
- Results predict observed drop in fluid permeability *k*.
- **Rigorous bound on *k* for bimodal distribution of pore sizes**

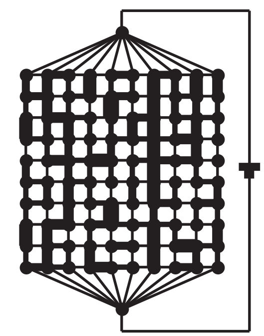

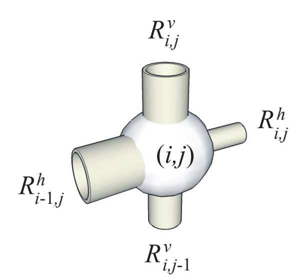

Steffen, Epshteyn, Zhu, Bowler, Deming, Golden 2017

Zhu, Jabini, Golden, Eicken, Morris *Ann. Glac.* 2006

How does the biology affect the physics?

Remote sensing of sea ice

INVERSE PROBLEM

Recover sea ice properties from electromagnetic (EM) data

$$\varepsilon^*$$

effective complex permittivity (dielectric constant, conductivity)

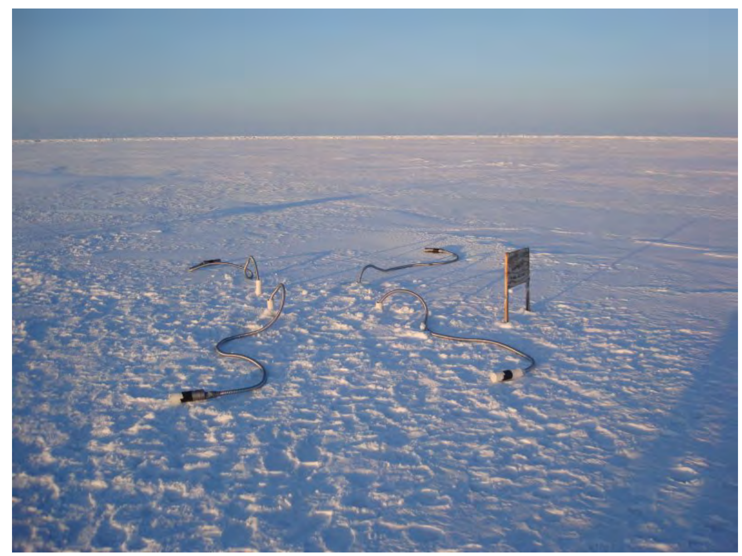

sea ice thickness
ice concentration

brine volume fraction
brine inclusion connectivity

Effective complex permittivity of a two phase composite in the quasistatic (long wavelength) limit

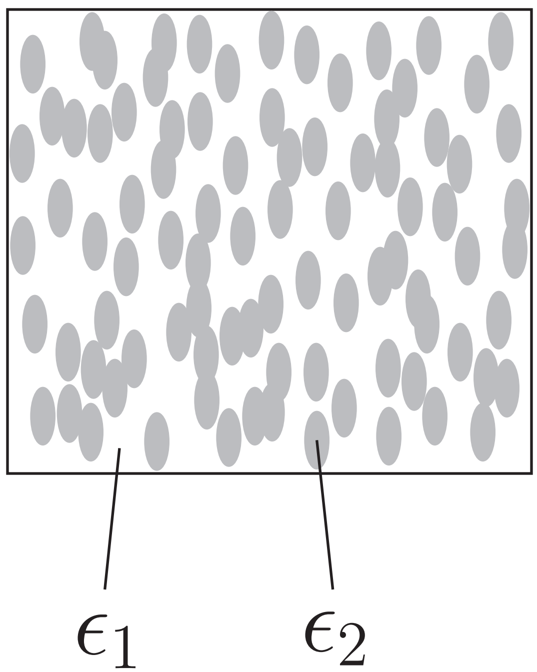

ϵ^*

$$D = \epsilon E$$

$$\nabla \cdot D = 0$$

$$\nabla \times E = 0$$

$$\langle D \rangle = \epsilon^* \langle E \rangle$$

p_1 , p_2 = volume fractions of the components

$$\epsilon^* = \epsilon^* \left(\frac{\epsilon_1}{\epsilon_2} \text{ , composite geometry} \right)$$

Theory of Effective Electromagnetic Behavior of Composites

analytic continuation method

Forward Homogenization Bergman (1978), Milton (1979), Golden and Papanicolaou (1983)
Theory of Composites, Milton (2002)

composite geometry
(spectral measure μ) ⟶ ε^*

integral representations, rigorous bounds, approximations, etc.

$$F(s) = 1 - \frac{\epsilon^*}{\epsilon_2} = \int_0^1 \frac{d\mu(z)}{s - z} \qquad s = \frac{1}{1 - \epsilon_1 / \epsilon_2}$$

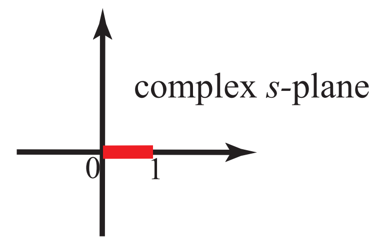

Inverse Homogenization Cherkaev and Golden (1998), Day and Thorpe (1999), Cherkaev (2001)
McPhedran, McKenzie, Milton (1982), *Theory of Composites*, Milton (2002)

ε^* ⟶ ***composite geometry***
(spectral measure μ)

recover brine volume fraction, connectivity, etc.

Stieltjes integral representation

separation of geometry from parameters

$$s = \frac{1}{1 - \epsilon_1 / \epsilon_2}$$

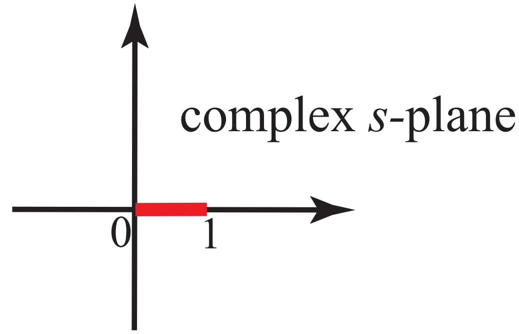

$$F(s) = 1 - \frac{\epsilon^*}{\epsilon_2} = \int_0^1 \frac{d\mu(z)}{s - z}$$

μ

- spectral measure of self adjoint operator $\Gamma\chi$
- mass $= p_1$
- higher moments depend on n-point correlations

$$\Gamma = \nabla(-\Delta)^{-1}\nabla\cdot$$

$\chi =$ characteristic function of the brine phase

$$E = (s + \Gamma\chi)^{-1} e_k$$

Golden and Papanicolaou, Comm. Math. Phys. 1983

forward and inverse bounds on the complex permittivity of sea ice

forward bounds

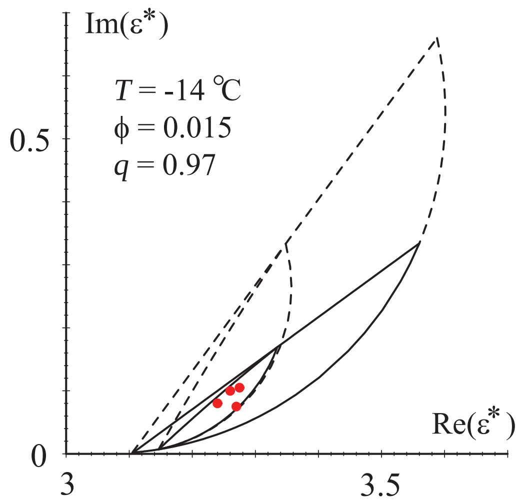

4.75 GHz data

matrix particle

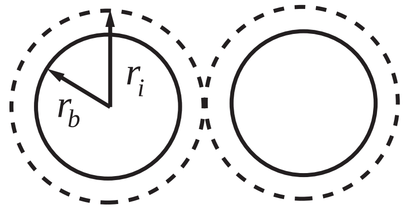

$$q = r_b / r_i$$

$$0 < q < 1$$

Golden 1995, 1997

Bruno 1991

inverse bounds and recovery of brine porosity

Gully, Backstrom, Eicken, Golden
Physica B, 2007

inverse bounds

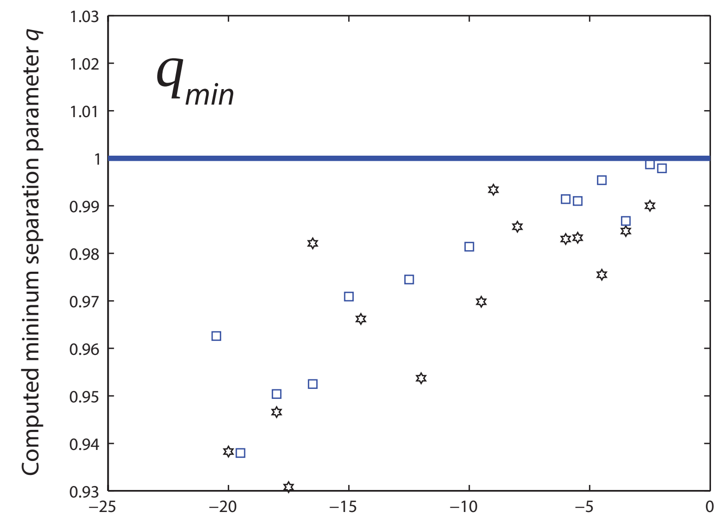

Slab temperature °C

inversion for brine inclusion separations in sea ice from measurements of effective complex permittivity ε^*

rigorous inverse bound on spectral gap

construct algebraic curves which bound admissible region in (p,q)-space

Orum, Cherkaev, Golden
Proc. Roy. Soc. A, 2012

the math doesn't care if it's sea ice or bone!

HUMAN BONE

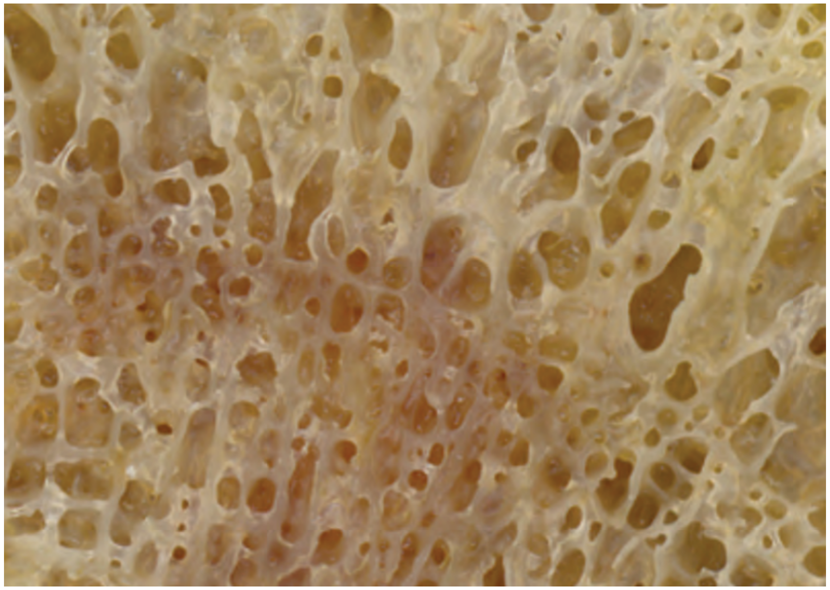

SEA ICE

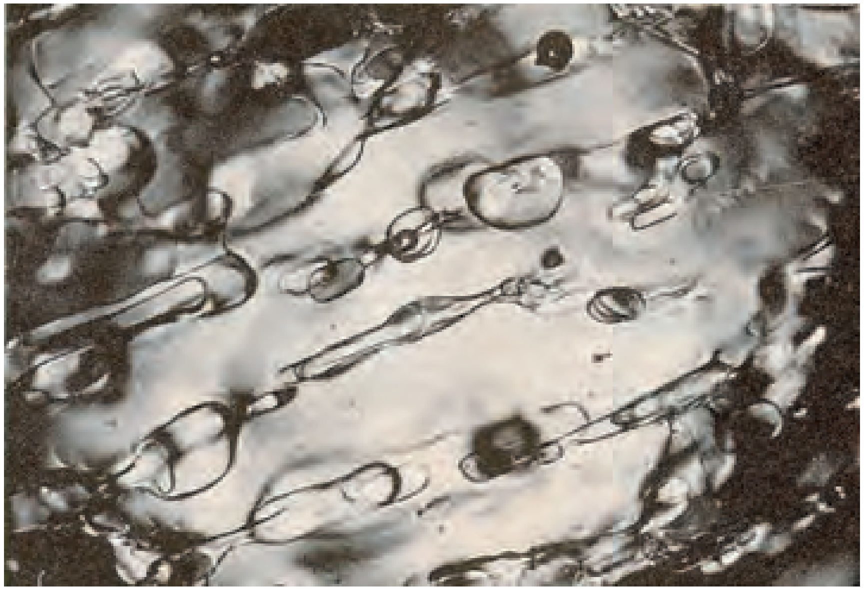

apply spectral measure analysis of brine connectivity and spectral inversion to electromagnetic monitoring osteoporosis

Golden, Murphy, Cherkaev, J. Biomechanics 2011

spectral characterization of porous microstructures in bone

Golden, Murphy, Cherkaev, J. Biomechanics 2011

(a) young healthy trabecular bone

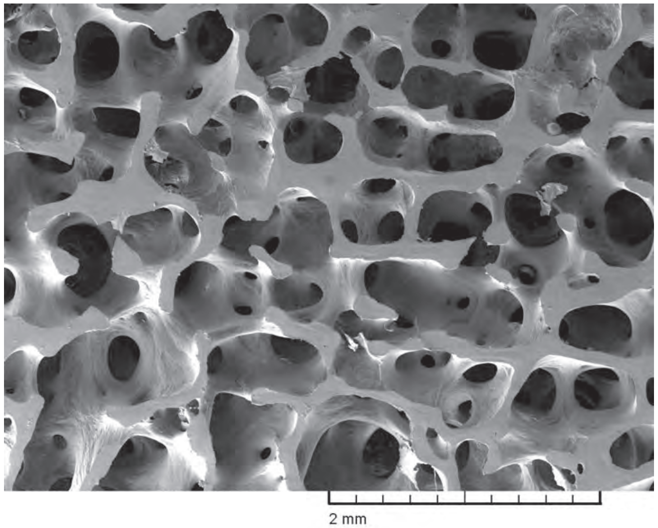

(b) old osteoporotic trabecular bone

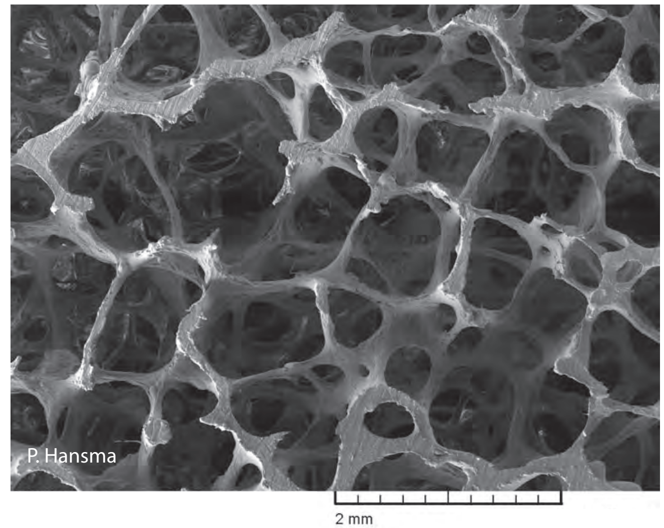

(c) spectral measure - young

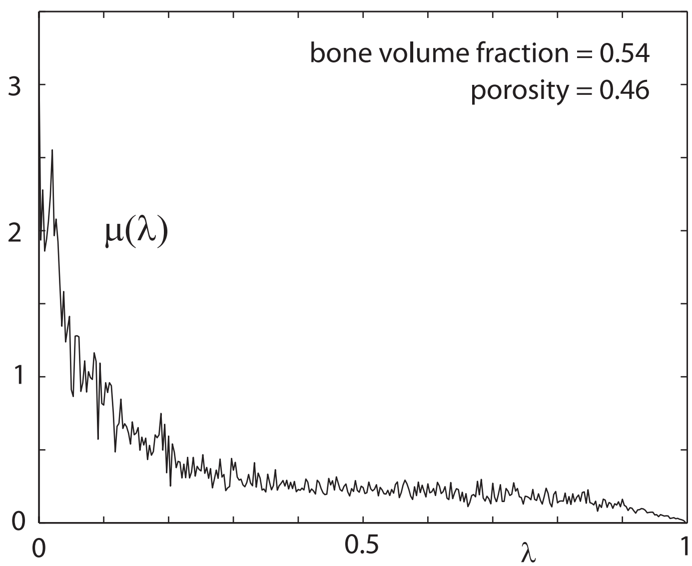

(d) spectral measure - old

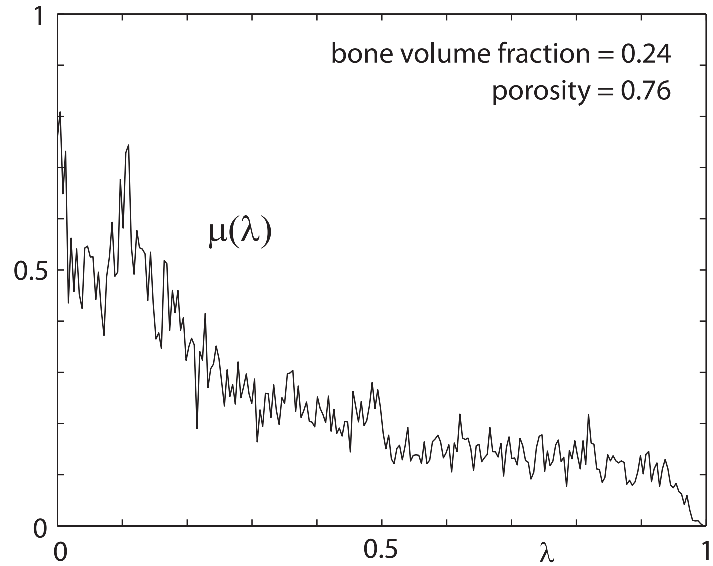

\+

reconstruction of spectral measures from complex permittivity data

using regularized inversion scheme

EM monitoring of osteoporosis

loss of bone connectivity

reconstruction of spectral measures from simulated complex permittivity data

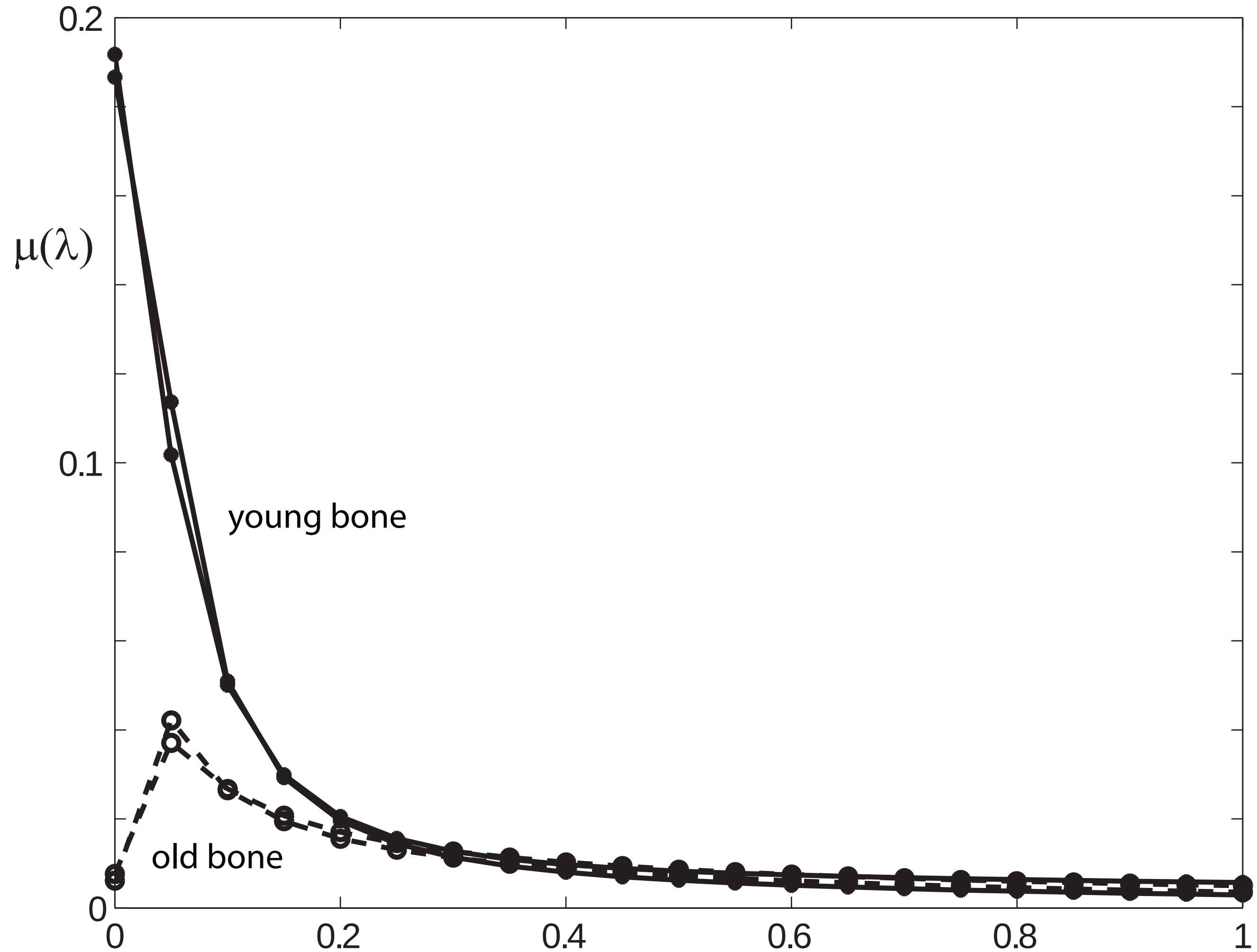

regularized inversion scheme

Golden, Murphy, Cherkaev, J. Biomech. 2011

direct calculation of spectral measure

1. Discretization of composite microstructure gives lattice of 1's and 0's (random resistor network).

2. The fundamental operator $\chi\Gamma\chi$ becomes a random matrix depending only on the composite geometry.

3. Compute the eigenvalues λ_i and eigenvectors of $\chi\Gamma\chi$ with inner product weights α_i

$$\mu(\lambda) = \sum_i \alpha_i \, \delta(\lambda - \lambda_i)$$

Dirac point measure (Dirac delta)

earlier studies of spectral measures

Day and Thorpe 1996
Helsing, McPhedran, Milton 2011

Continuum composite

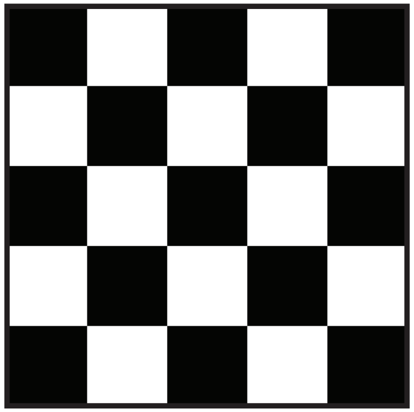

Spectral measures of

$$\chi_1 \Gamma \chi_1$$

Murphy, Hohenegger, Cherkaev, Golden
Comm. Math. Sci. 2015

Discrete composite

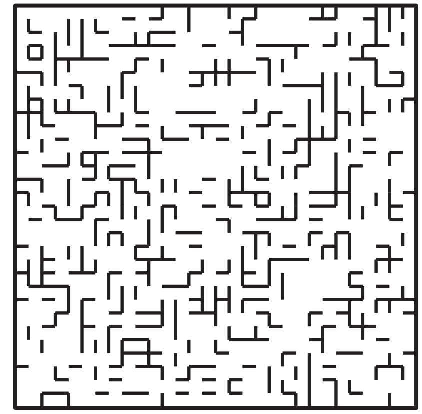

Integro-differential projection operator

$$\Gamma = \vec{\nabla}(\Delta^{-1})\vec{\nabla}\cdot$$

Point-wise indicator function

$$\chi_1$$

Resolvent representation of electric field

$$\chi_1 \vec{E} = sE_0(sI - \chi_1 \Gamma \chi_1)^{-1} \chi_1 \vec{e}_k$$

Integral representation

$$F(s) = \int_0^1 \frac{d\mu(\lambda)}{s - \lambda}$$

Projection matrix

$$\Gamma = \nabla(\nabla^{\mathrm{T}} \nabla)^{-1} \nabla^{\mathrm{T}}$$

Diagonal projection matrix

$$\chi_1$$

Series representation of electric field

$$\chi_1 \vec{E} = sE_0 \sum_j \frac{\vec{v}_j \cdot \chi_1 \vec{e}_k}{s - \lambda_j} \vec{v}_j$$

Series representation

$$F(s) = \sum_j \frac{(\vec{v}_j \cdot \chi_1 \vec{e}_k)^2}{s - \lambda_j}$$

Spectral statistics for 2D random resistor network

Log Electric Field

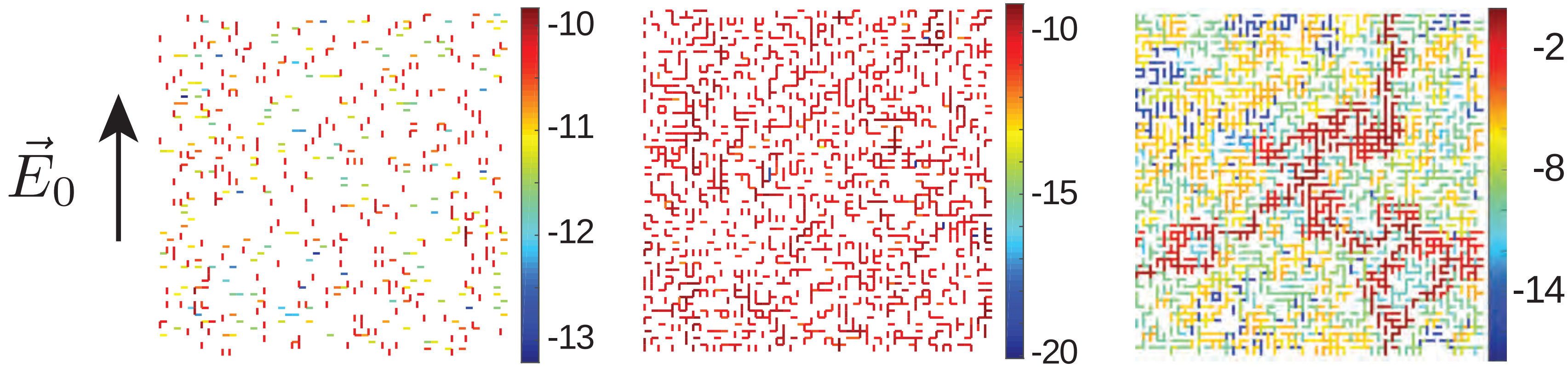

Murphy and Golden, J. Math. Phys., 2012

Murphy et al. Comm. Math. Sci., 2015

Spectral Measures

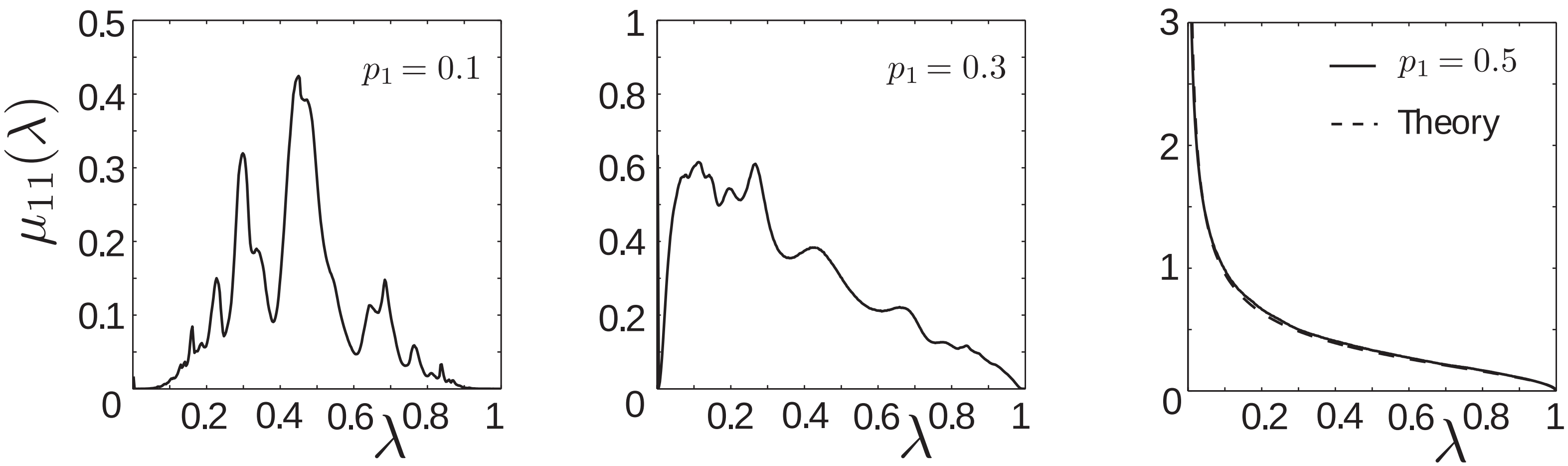

Eigenvalue Spacing Distributions

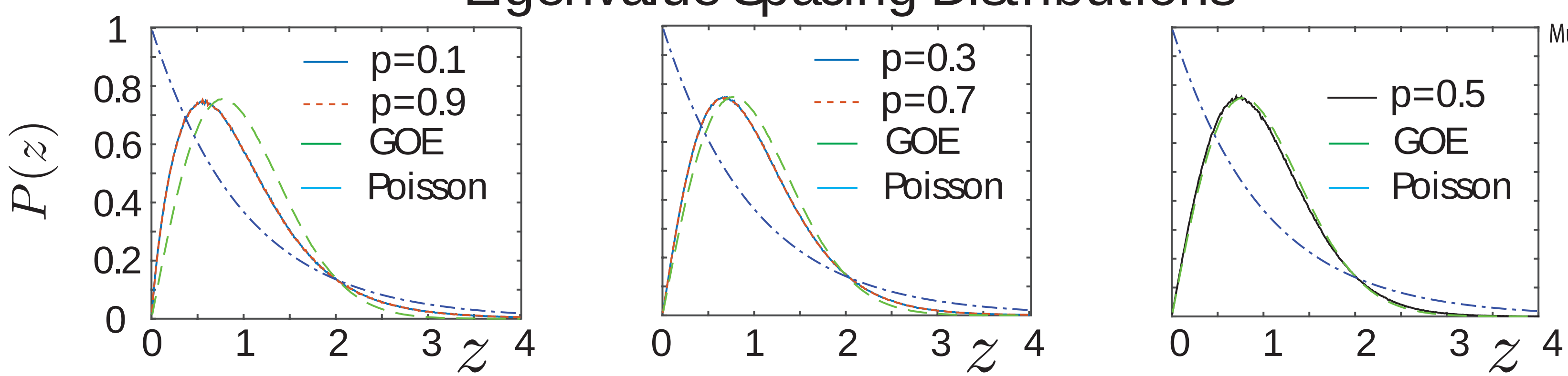

Murphy, Cherkaev, Golden, 2016

Eigenvalue Statistics of Random Matrix Theory

Wigner (1951) and Dyson (1953) first used random matrix theory (RMT) to describe quantized energy levels of heavy atomic nuclei.

$[\mathbf{N}]_{ij} \sim N(0,1),$ $\mathbf{A} = (\mathbf{N}+\mathbf{N}^T)/2$ ***Gaussian orthogonal ensemble (GOE)***

$[\mathbf{N}]_{ij} \sim N(0,1)+iN(0,1),$ $\mathbf{A} = (\mathbf{N}+\mathbf{N}^{\dagger})/2$ ***Gaussian unitary ensemble (GUE)***

Short range and long range correlations of eigenvalues are measured by various eigenvalue statistics

Spacing distributions of energy levels for heavy atomic nuclei

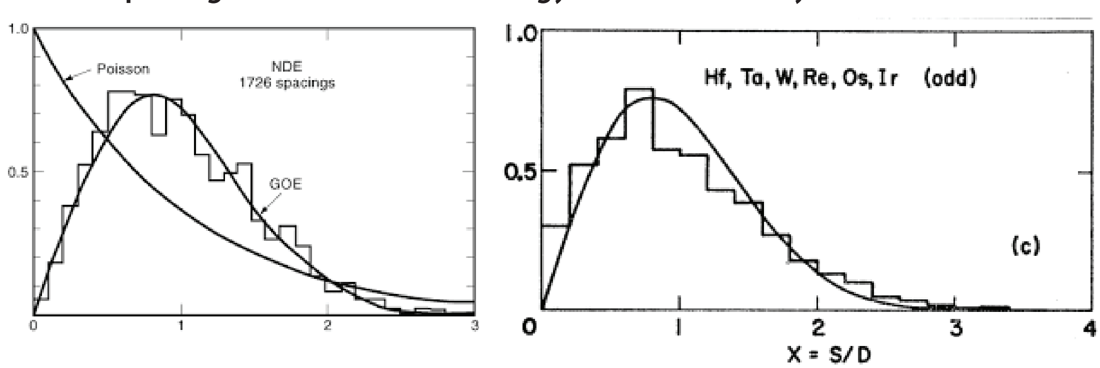

Spacing distributions of the first billion zeros of the Riemann zeta function

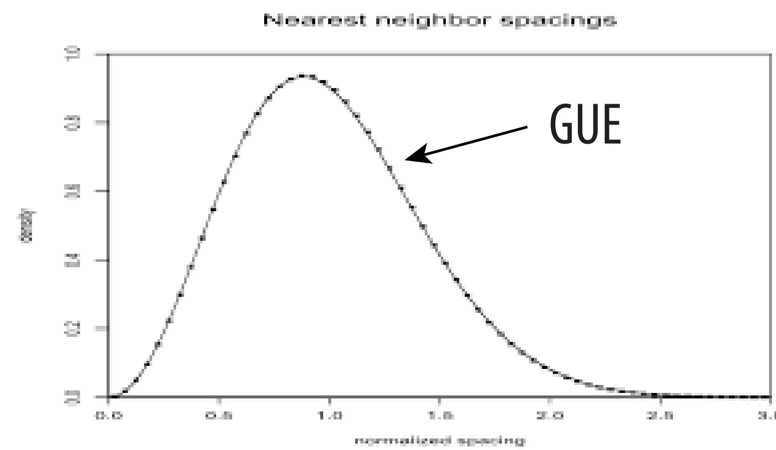

RMT used to characterize disorder-driven transitions in mesoscopic conductors, neural networks, random graph theory, etc.

Phase transitions ~ transitions in universal eigenvalue statistics.

Spectral computations for Arctic melt ponds

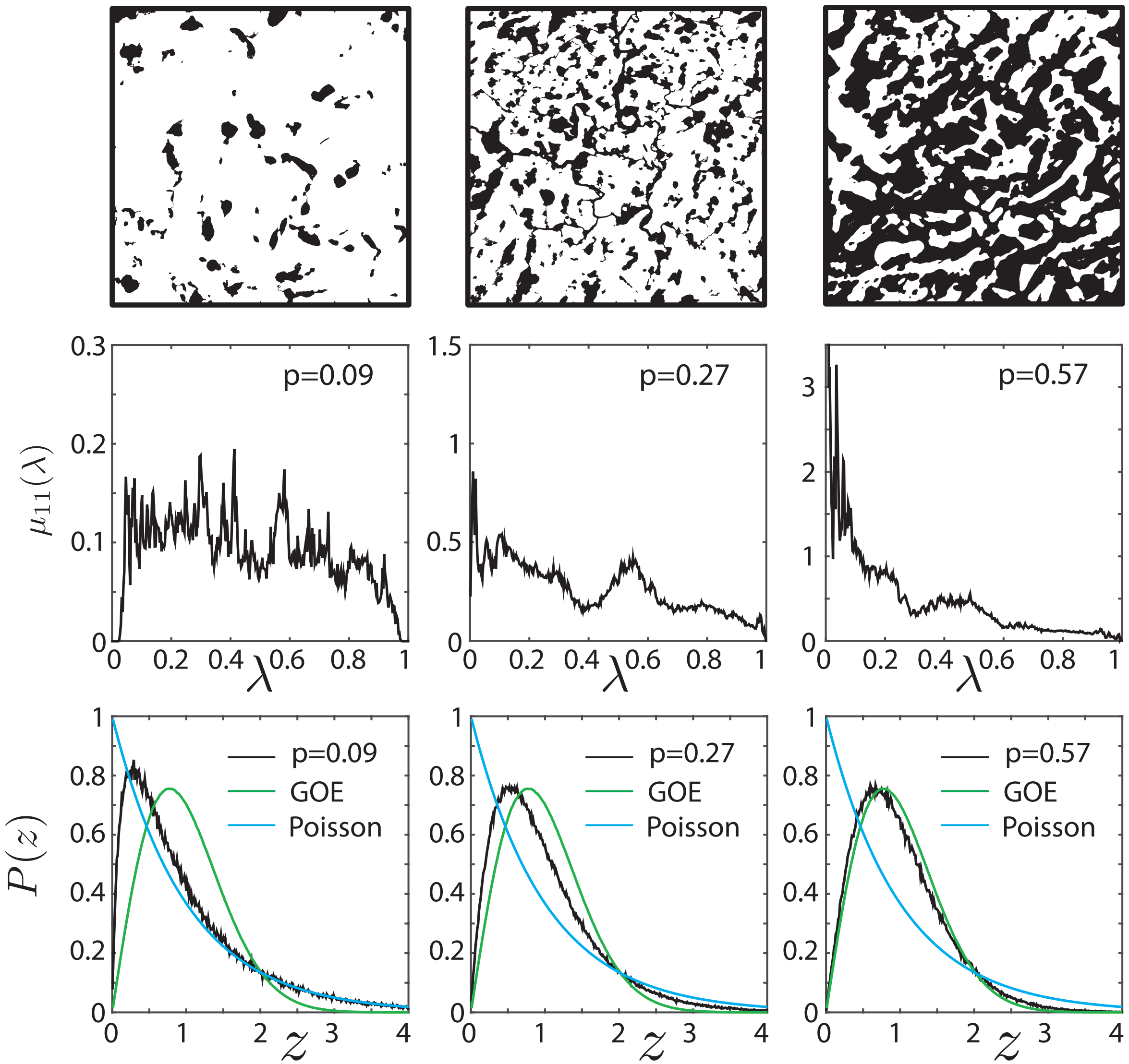

spectral measures

eigenvalue spacing distributions

uncorrelated → **level repulsion**

TRANSITION

Ben Murphy
Elena Cherkaev
Ken Golden
2017

eigenvalue statistics for transport tend toward the UNIVERSAL Wigner-Dyson distribution as the "conducting" phase percolates

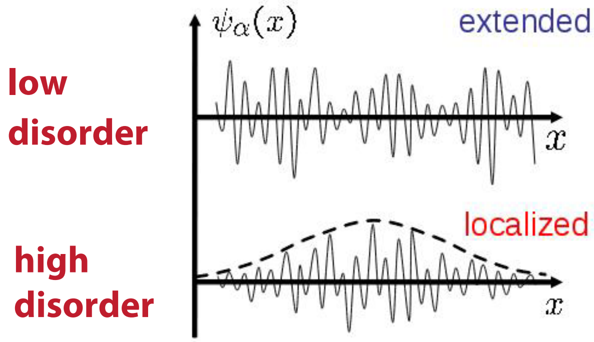

metal / insulator transition

localization

Anderson 1958
Mott 1949
Shklovshii et al 1993
Evangelou 1992

Anderson transition in wave physics:
quantum, optics, acoustics, water waves, ...

we find a surprising analog

Anderson transition for classical transport in composites

Murphy, Cherkaev, Golden Phys. Rev. Lett. 2017

PERCOLATION TRANSITION → **transition to universal eigenvalue statistics (GOE) extended states, mobility edges**

-- but without wave interference or scattering effects ! --

eigenvector localization and mobility edges

Inverse Participation Ratio: $I(\vec{v}_n) = \sum_{i=1}^{N} |(\vec{v}_n)_i|^4$

Completely Localized: $I(\vec{e}_n) = 1$

Completely Extended: $I\left(\frac{1}{\sqrt{N}}\vec{1}\right) = \frac{1}{N}$

Anderson Model

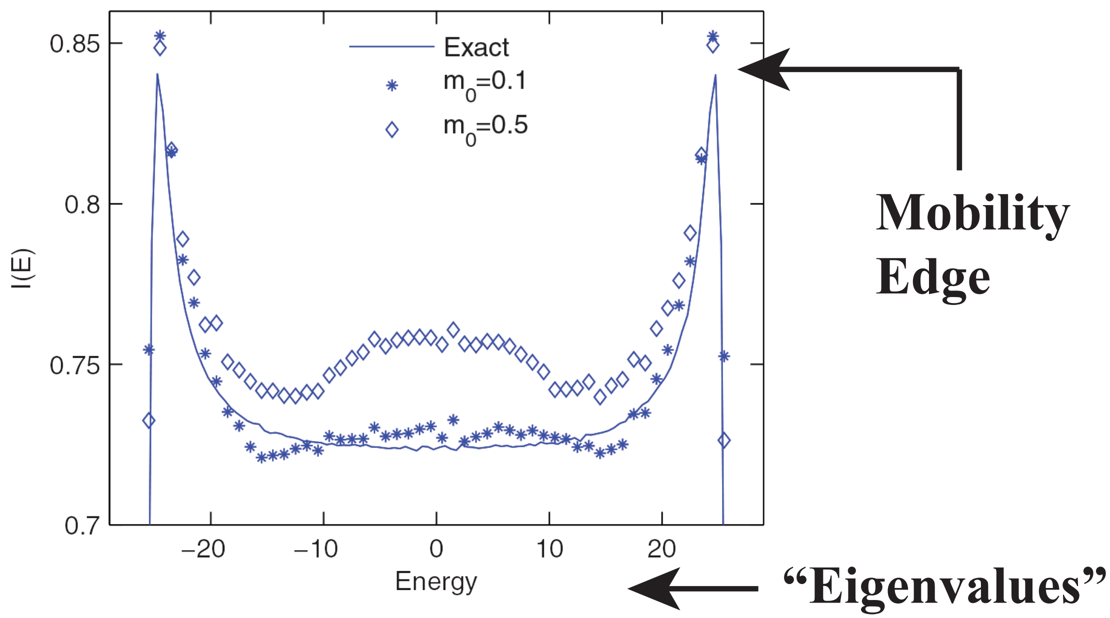

FIG. 4. (Color online) IPR for Anderson model in two dimensions with $x = 6.25$ ($w = 50$) from exact diagonalization (solid line) and from LDRG with different values of the cutoff m_0. LDRG data are averaged over 100 runs of systems with 100×100 sites.

PHYSICAL REVIEW B 90, 060205(R) (2014)

Localization properties of eigenvectors in random resistor networks

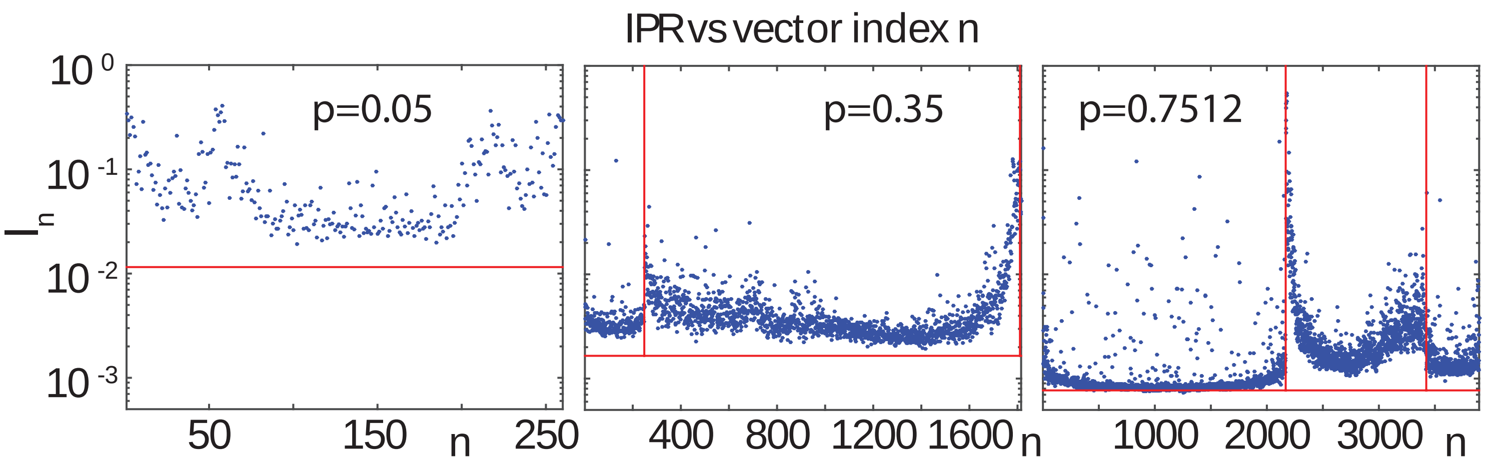

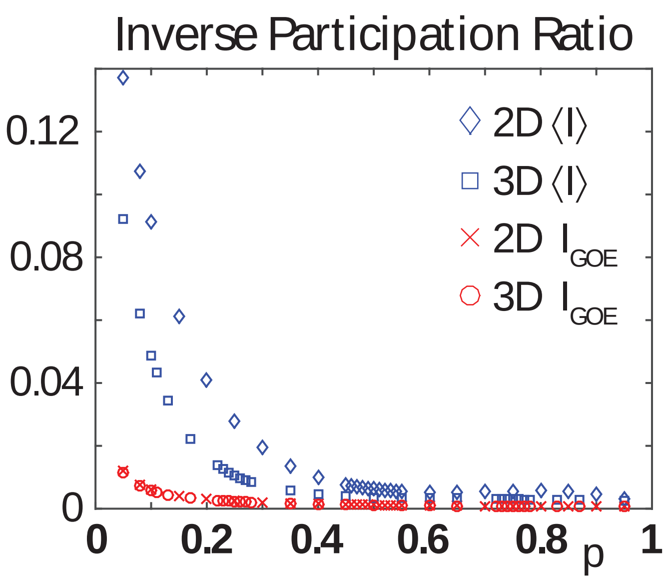

$$I_n = \sum_i (\vec{v}_n)_i^4$$

Murphy, Cherkaev, Golden, 2017

Homogenization for composite materials

Two-component composites

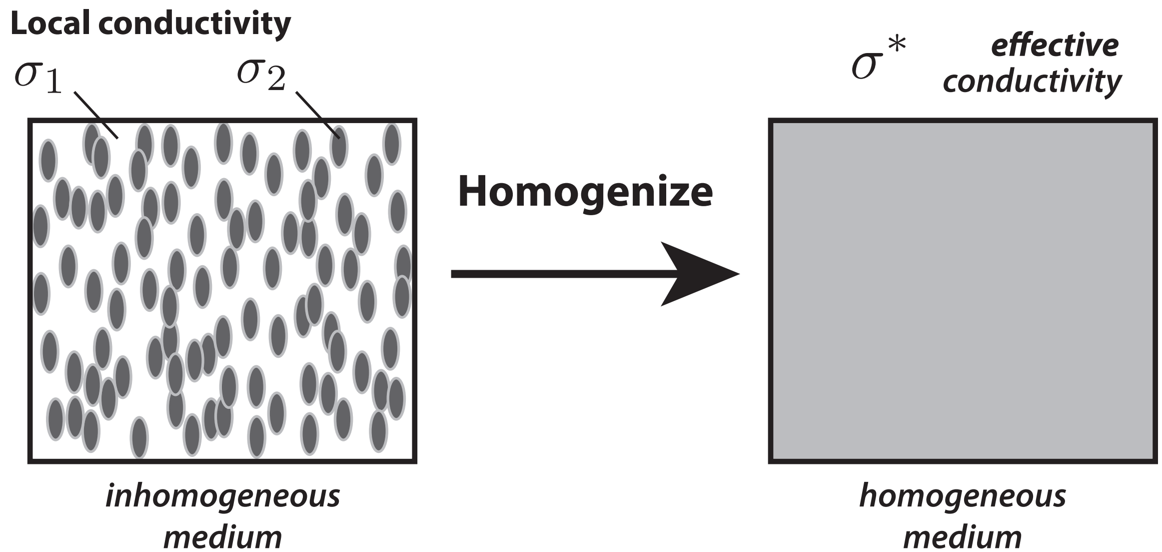

Find the homogeneous medium which behaves macroscopically the same as the inhomogeneous medium

Polycrystalline media

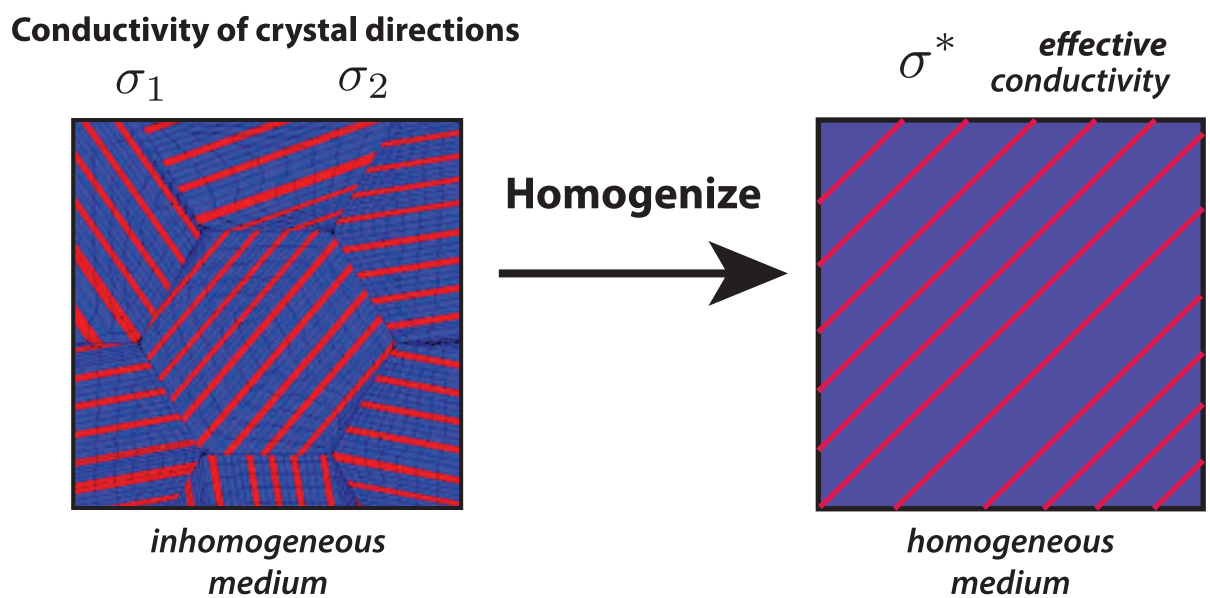

Bounds on the complex permittivity of polycrystalline materials by analytic continuation

Adam Gully, Joyce Lin,
Elena Cherkaev, Ken Golden

- **Stieltjes integral representation for effective complex permittivity**

  Milton (1981, 2002), Barabash and Stroud (1999), ...
- **Forward and inverse bounds**
- **Applied to sea ice using two-scale homogenization**
- **Inverse bounds give method for distinguishing ice types using remote sensing techniques**

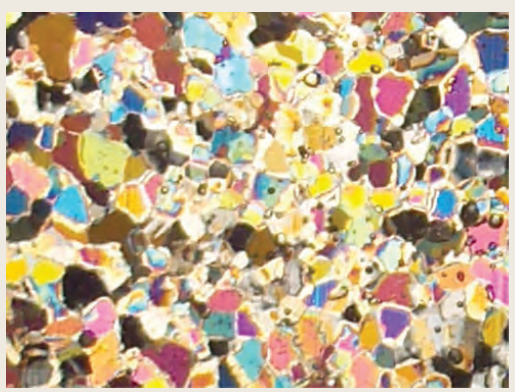

Proc. Roy. Soc. A   8 Feb 2015

Proc. R. Soc. A | Volume 471 | Issue 2174 | 8 February 2015

ISSN 1364-5021 | Volume 471 | Issue 2174 | 8 February 2015

PROCEEDINGS A

350 YEARS OF SCIENTIFIC PUBLISHING

An invited review commemorating 350 years of scientific publishing at the Royal Society

A method to distinguish between different types of sea ice using remote sensing techniques

A computer model to determine how a human should walk so as to expend the least energy

two scale homogenization for polycrystalline sea ice

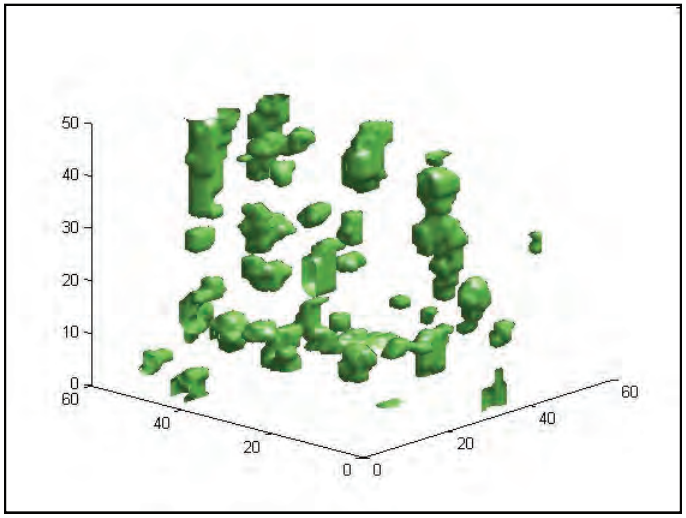

numerical homogenization for single crystal

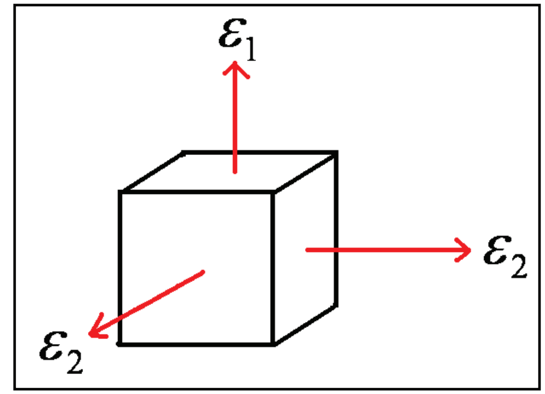

analytic continuation for polycrystals

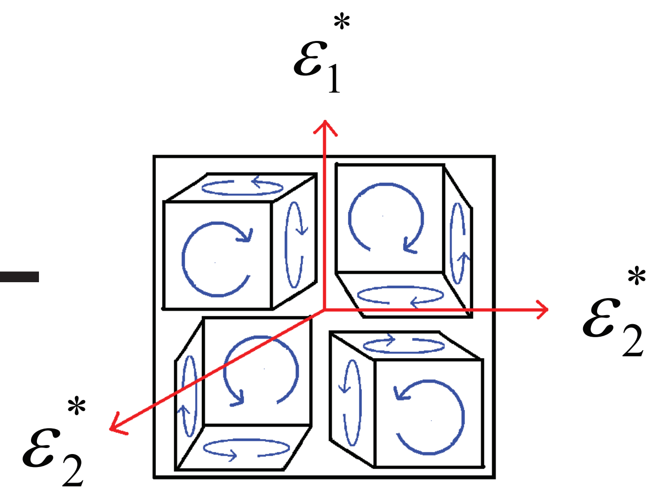

bounds

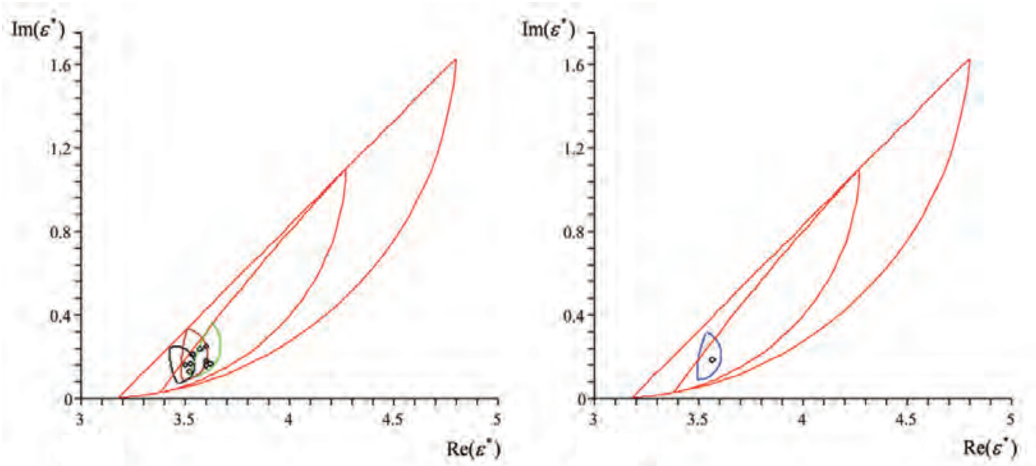

Gully, Lin, Cherkaev, Golden, Proc. Roy. Soc. A (and cover) 2015

advection enhanced diffusion

effective diffusivity

tracers, buoys diffusing in ocean eddies
diffusion of pollutants in atmosphere
salt and heat transport in ocean
heat transport in sea ice with convection

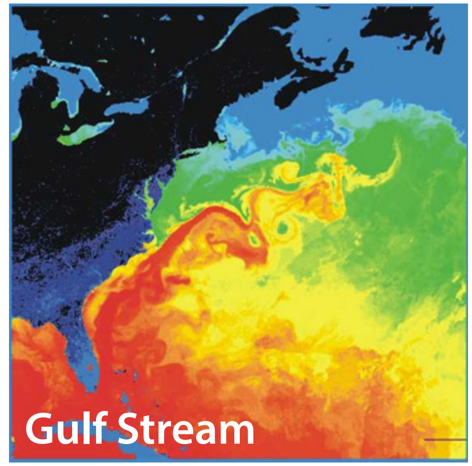

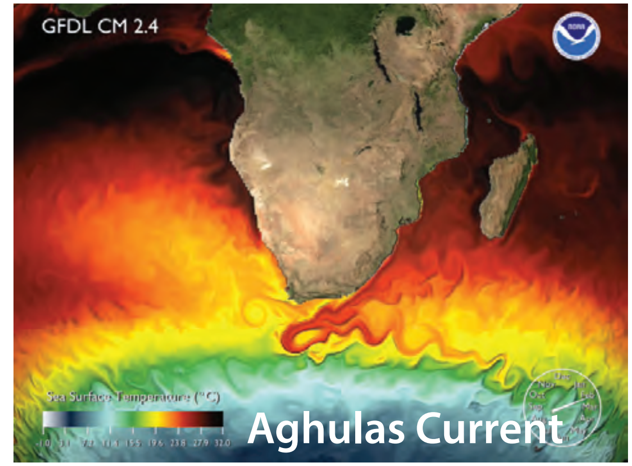

advection diffusion equation with a velocity field $\vec{u}$

$$\frac{\partial T}{\partial t} + \vec{u} \cdot \vec{\nabla} T = \kappa_0 \Delta T$$

$$\vec{\nabla} \cdot \vec{u} = 0$$

↓ ***homogenize***

$$\frac{\partial \overline{T}}{\partial t} = \kappa^* \Delta \overline{T}$$

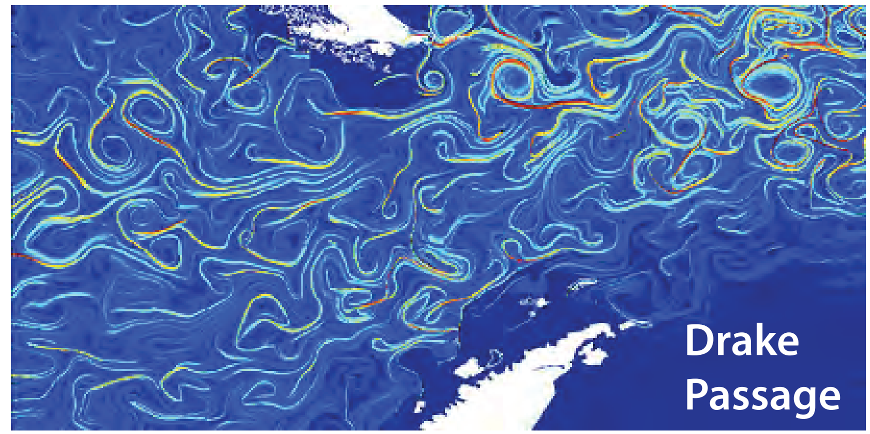

κ^* *effective diffusivity*

Stieltjes integral for κ^* *with spectral measure*

Avellaneda and Majda, PRL 89, CMP 91

Murphy, Cherkaev, Xin, Zhu, Golden, *Ann. Math. Sci. Appl.* 2017
Murphy, Cherkaev, Zhu, Xin, Golden, 2017

Spectral measures and eigenvalue spacings for cat's eye flow

$$H(x,y) = \sin(x)\sin(y) + A\cos(x)\cos(y), \qquad A \sim U(-p,p)$$

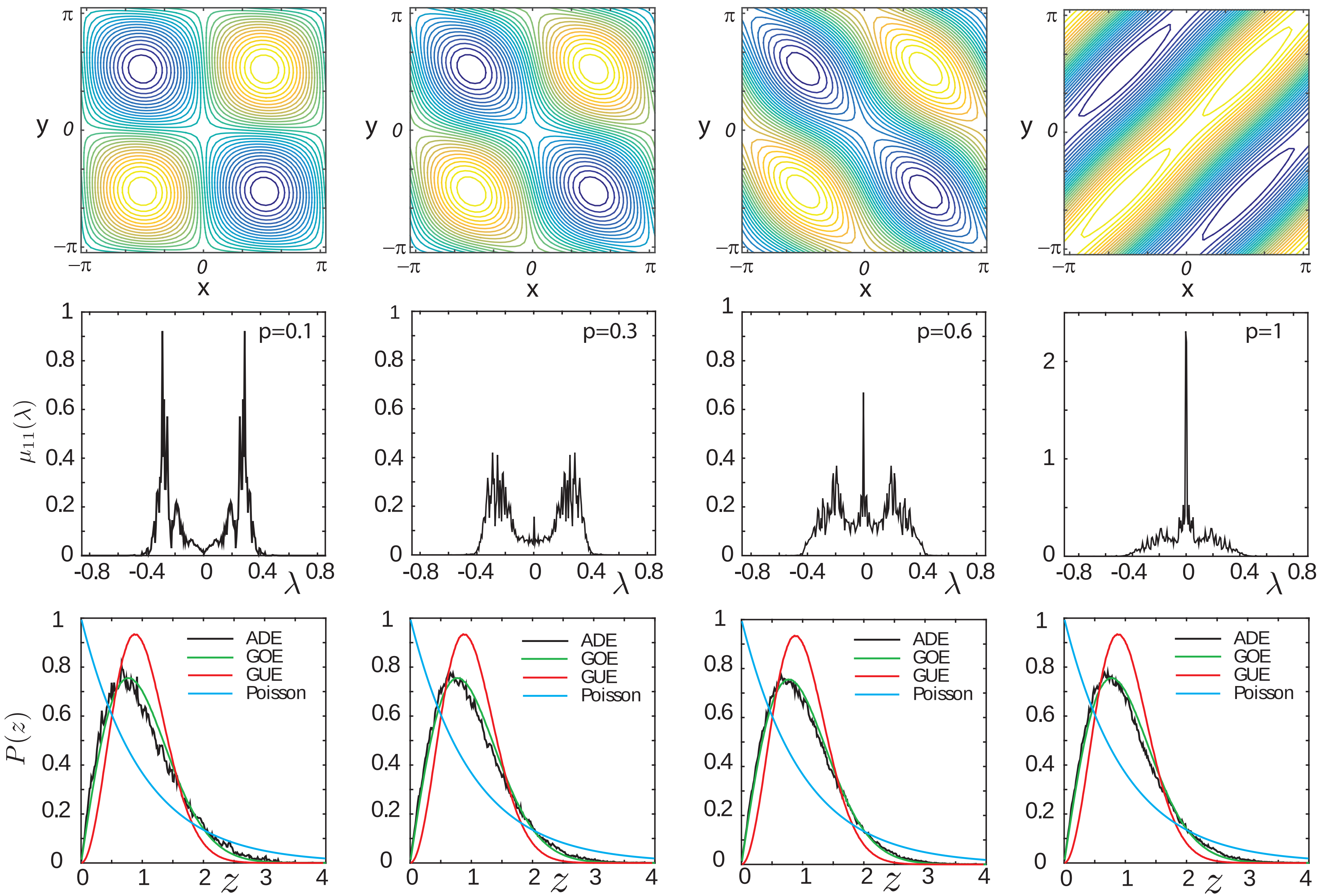

Murphy, Cherkaev, Xin, Golden, 2017

Convection - enhanced thermal conductivity of sea ice w/ BC - flow

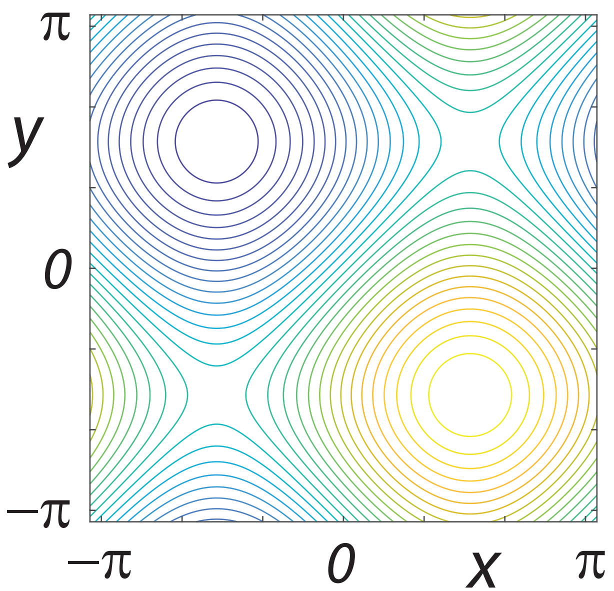

BC **- flow streamlines**

$H = B \sin x - C \sin y \quad B = C$

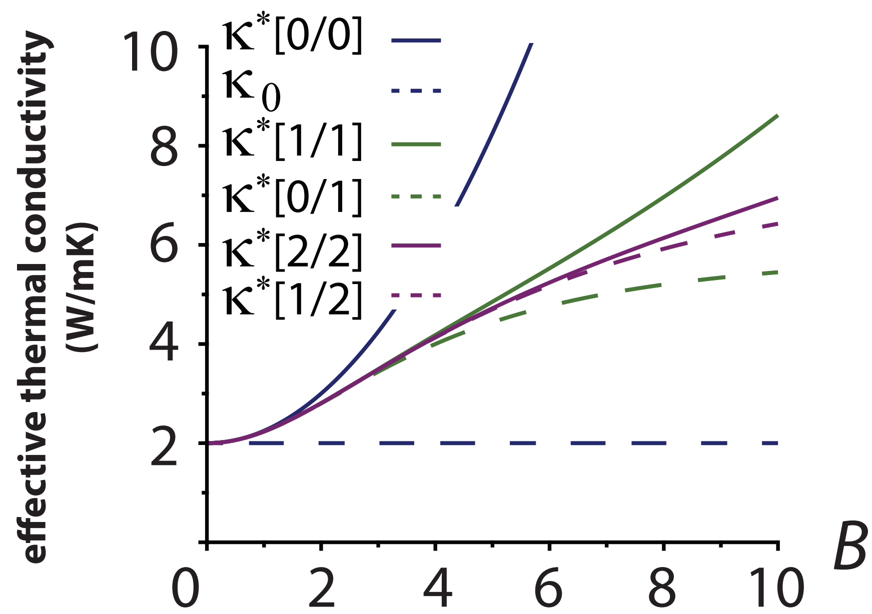

rigorous Padé bounds from Stieltjes integral + analytical calculations of moments of measure

Kraitzman, Hardenbrook, Murphy, Zhu, Cherkaev, Golden 2017

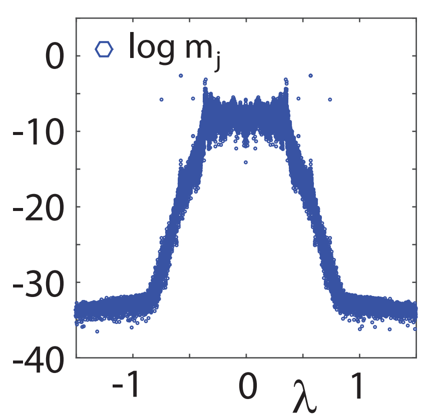

spectral masses

Murphy, Cherkaev, Zhu, Xin, Golden 2017

Storm-induced sea-ice breakup and the implications for ice extent

Kohout et al., *Nature* 2014

- during three large-wave events, significant wave heights did not decay exponentially, enabling large waves to persist deep into the pack ice.

- large waves break sea ice much farther from the ice edge than would be predicted by the commonly assumed exponential decay

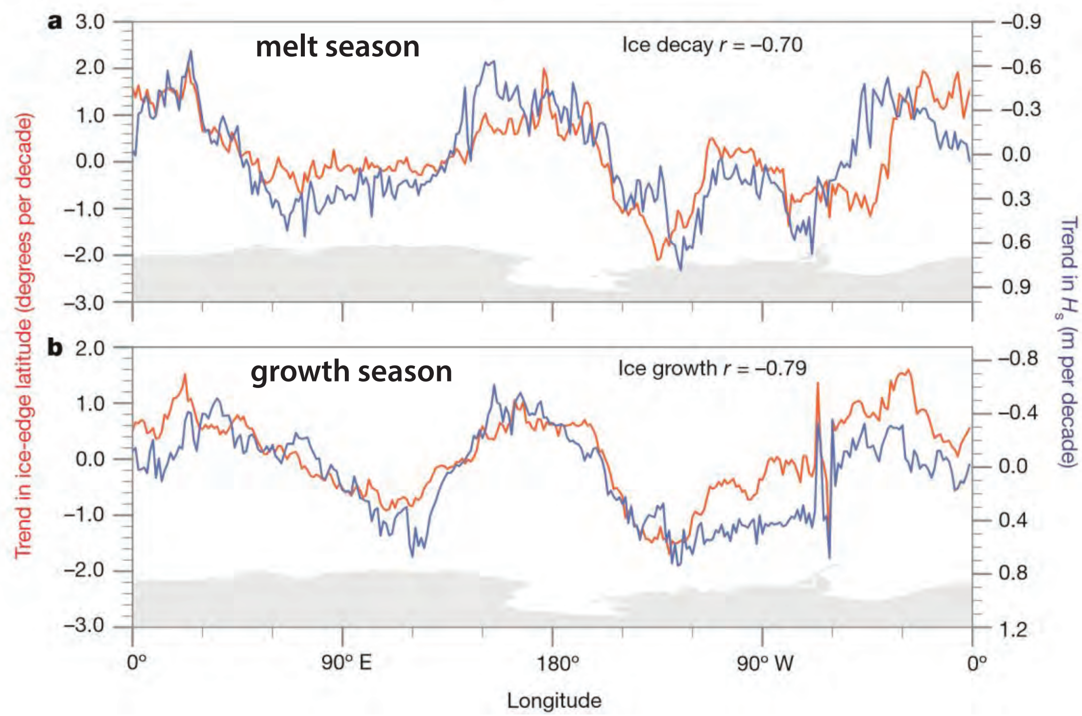

ice extent compared with significant wave height

Waves have strong influence on both the floe size distribution and ice extent.

Two Layer Models and Effective Parameters

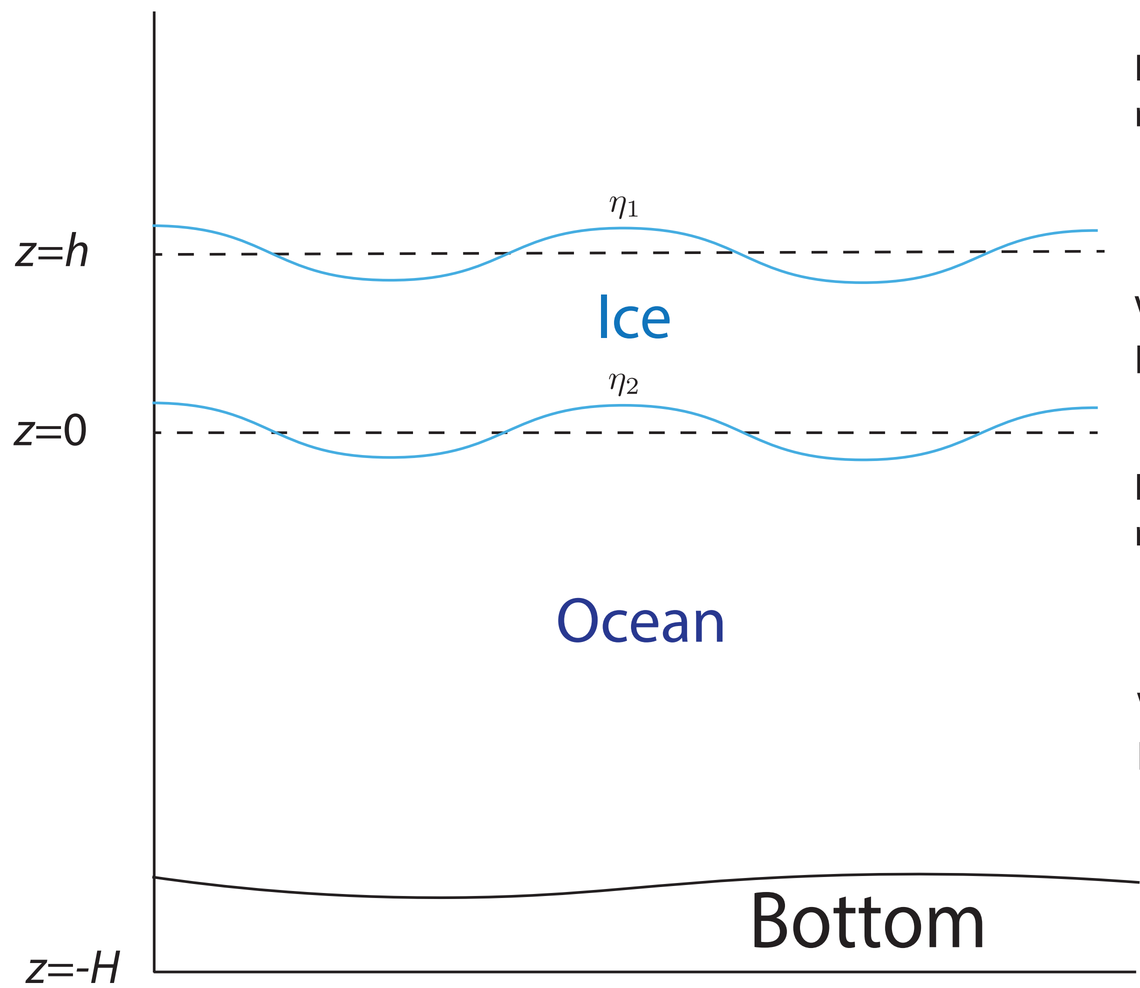

G shear modulus P pressure ω angular frequency U velocity field

ν viscosity λ Poission ratio ρ density g gravity

Viscous fluid layer (Keller 1998)
Effective Viscosity ν

Equations of motion:

$$\frac{\partial U}{\partial t} = -\frac{1}{\rho}\nabla P + \nu\nabla^2 U + g$$

Viscoelastic fluid layer (Wang-Shen 2010)
Effective Complex Viscosity $\nu_e = \nu + iG/\rho\omega$

Equations of motion

$$\frac{\partial U}{\partial t} = -\frac{1}{\rho}\nabla P + \nu_e\nabla^2 U + g$$

Viscoelastic thin beam (Mosig *et al.* 2015)
Effective Complex Shear Modulus $G_v = G - i\omega\rho\nu$

Stieltjes integral representation for effective complex viscoelastic parameter; bounds

Sampson, Murphy, Golden 2017

wave propagation in the marginal ice zone

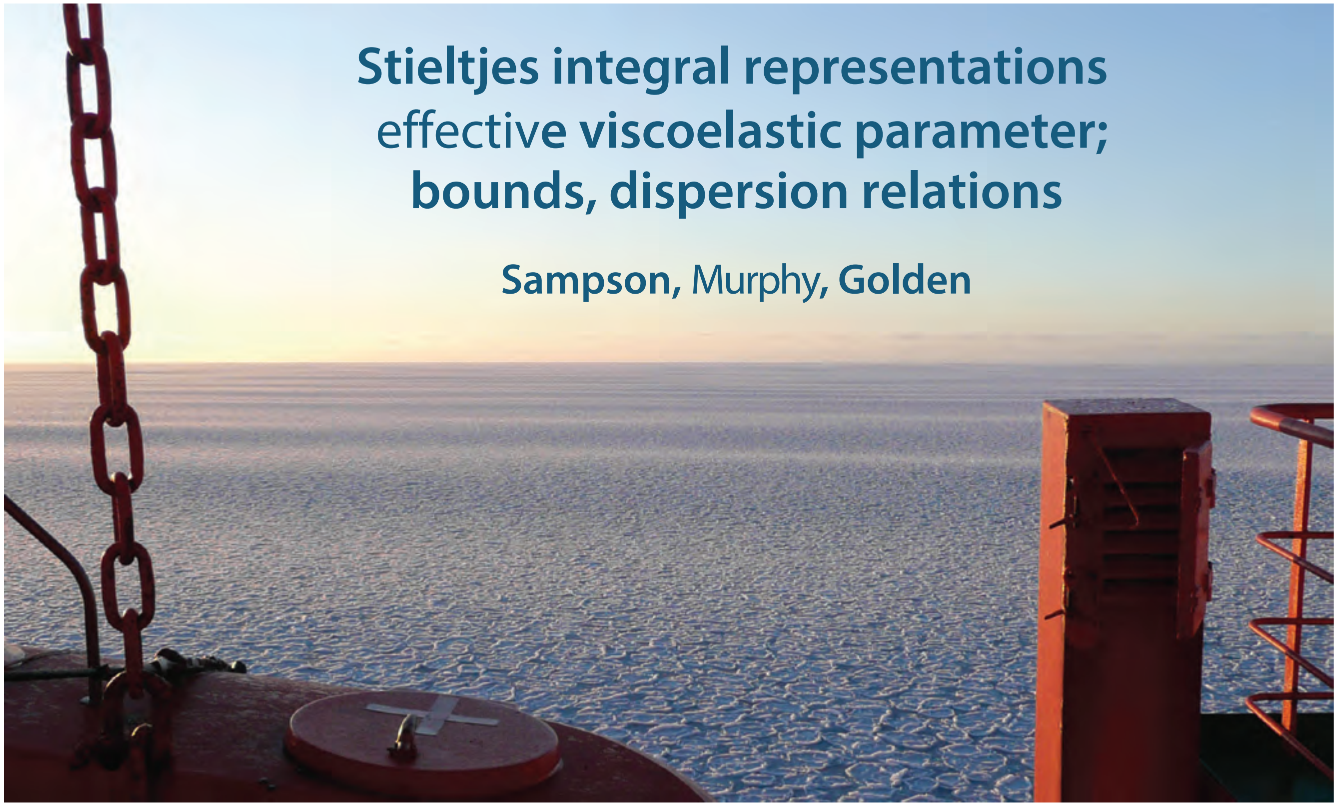

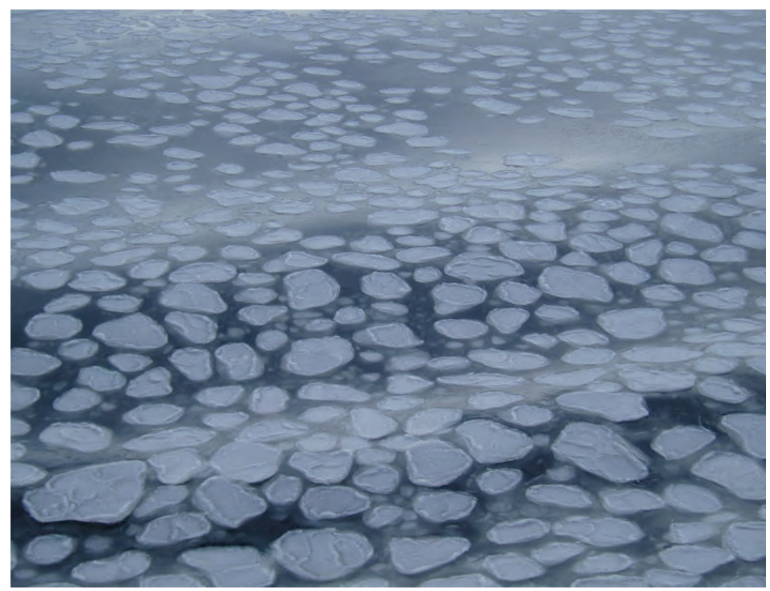

Stieltjes Integral Representation for Complex Viscoelasticity

$$\nabla \cdot \sigma = 0 \qquad \sigma_{ij} = C_{ijkl}\epsilon_{kl} \qquad \langle\sigma_{ij}\rangle = C^*_{ijkl}\langle\epsilon_{kl}\rangle$$

local $$C_{ijkl} = (\nu_1\chi + (1-\chi)\nu_2)\lambda_s$$

$$\nabla \cdot \big((\nu_1\chi + (1-\chi)\nu_2)\lambda_s : \epsilon\big) = 0$$

$$s = \frac{1}{1 - \frac{\nu_1}{\nu_2}}$$

Strain Field

$$\epsilon = \frac{1}{2}[\nabla u + (\nabla u)^T] = \nabla^s u$$

$\epsilon = \epsilon_0 + \epsilon_f$ where $\epsilon_f = \nabla^s \phi$

Elasticity Tensor

$$C^*_{ijkl} = \nu^*\left(\delta_{ik}\delta_{jl} + \delta_{il}\delta_{jk} - \frac{2}{3}\delta_{ij}\delta_{kl}\right) = \nu^*\lambda_s$$

RESOLVENT $$\epsilon = \left(1 - \frac{1}{s}\Gamma\chi\right)^{-1}\epsilon_0 \qquad \Gamma = \nabla^s(\nabla\cdot\nabla^s)^{-1}\nabla\cdot$$

ϵ_0 **avg strain**

$$F(s) = 1 - \frac{\nu^*}{\nu_2} \qquad F(s) = ||\epsilon_0||^{-2}\int_\Sigma \frac{d\mu(\lambda)}{s-\lambda}$$

bounds on the effective complex viscoelasticity

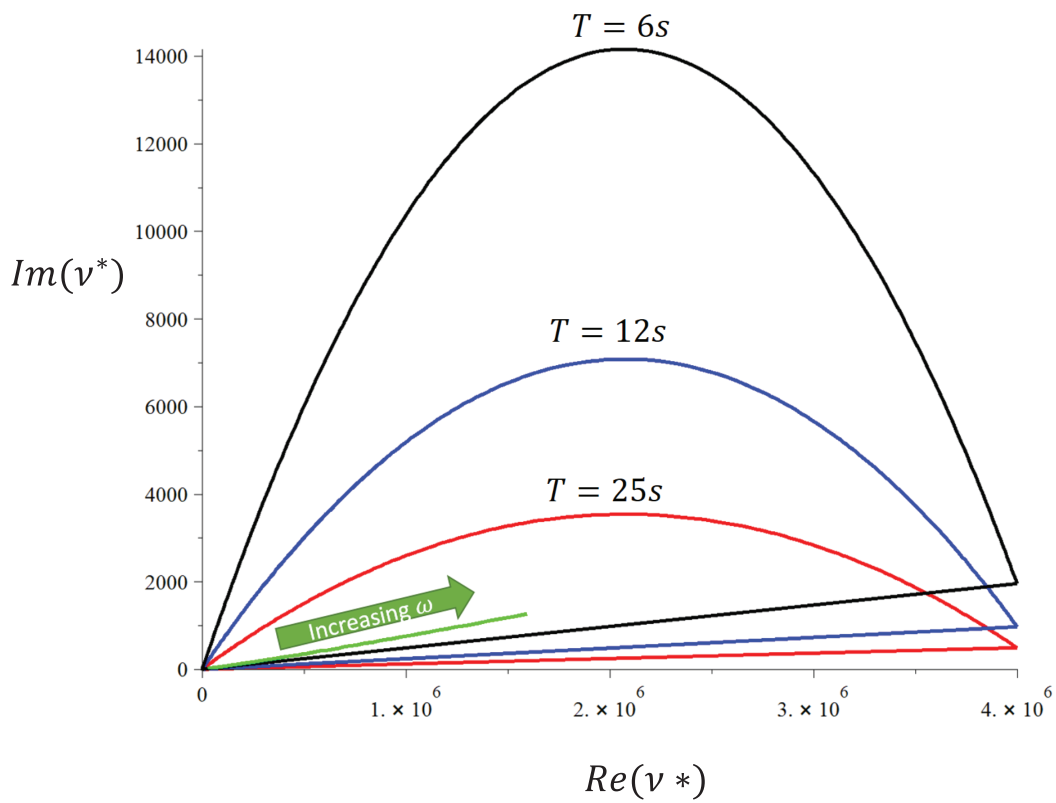

complex elementary bounds (fixed area fraction of floes)

$\nu_1 = 10^7 + i\,4875$ **pancake ice**

$\nu_2 = 5 + i\,0.0975$ **slush / frazil**

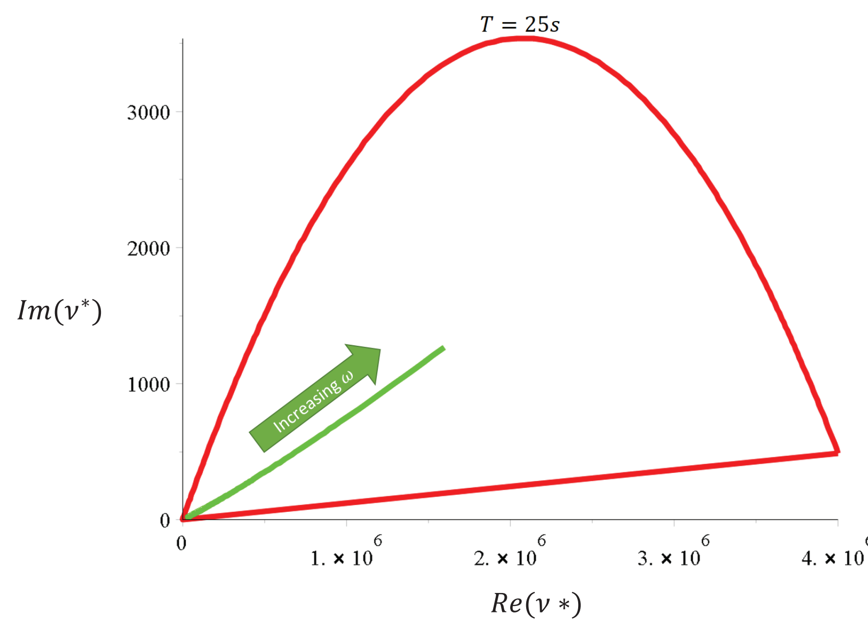

Sampson, Murphy, Golden 2017

Objective method for measuring MIZ width motivated by medical imaging and diagnostics

Strong, *Climate Dynamics* 2012
Strong and Rigor, *GRL* 2013

39% widening
1979 - 2012

streamlines of a solution to Laplace's equation

"average" lengths of streamlines

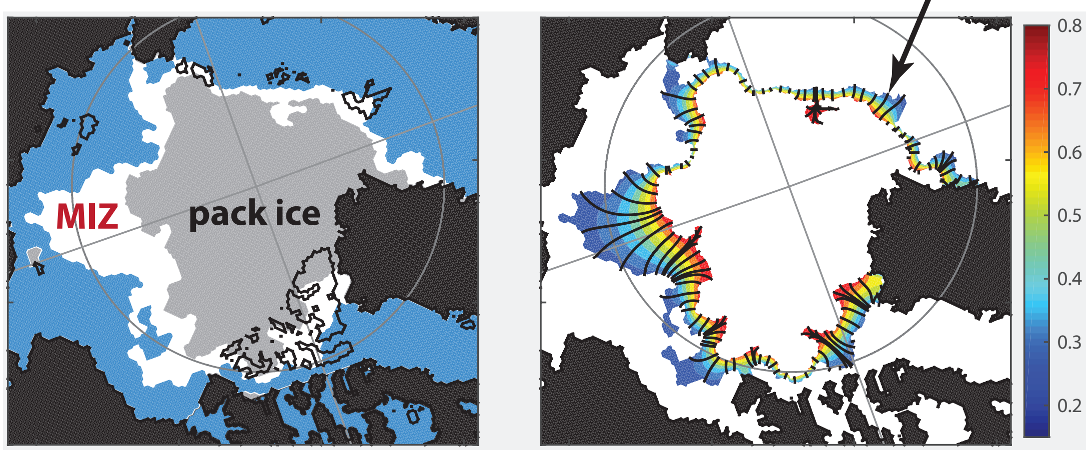

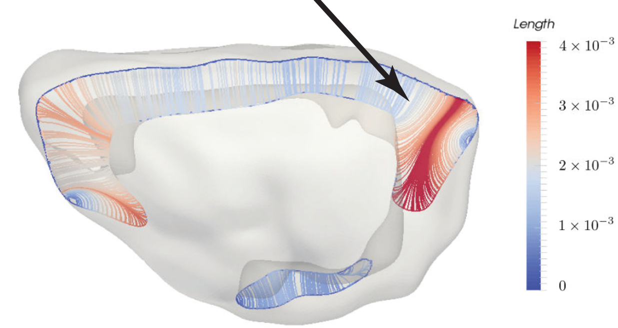

Arctic Marginal Ice Zone

crossection of the cerebral cortex of a rodent brain

analysis of different MIZ WIDTH definitions

Strong, Foster, Cherkaev, Eisenman, Golden
J. Atmos. Oceanic Tech. 2017

Strong and Golden
Society for Industrial and Applied Mathematics News, April 2017

Filling the polar data gap

hole in satellite coverage
of sea ice concentration field

previously assumed ice covered

Gap radius: 611 km
06 January 1985

Gap radius: 311 km
30 August 2007

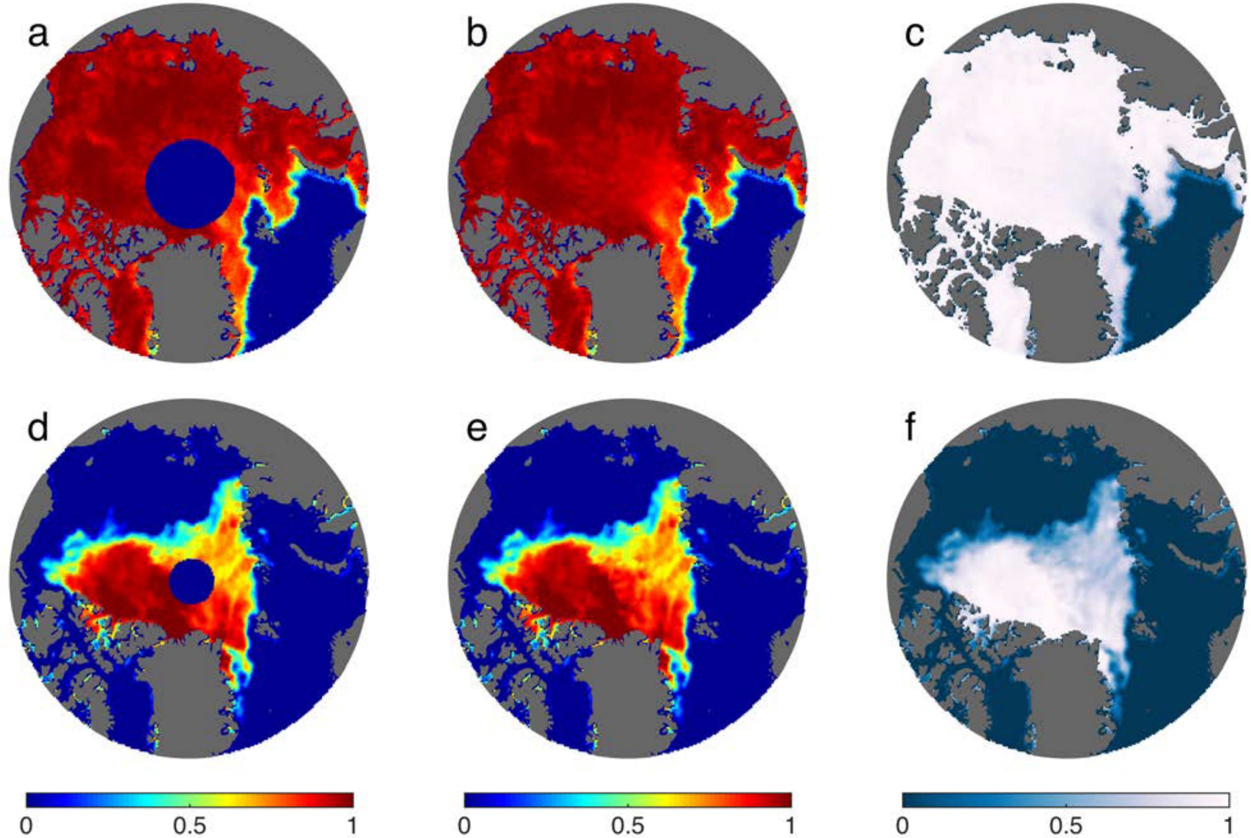

fill with harmonic function satisfying satellite BC's plus stochastic term

Strong and Golden, *Remote Sensing* 2016
Strong and Golden, *SIAM News* 2017

Arctic and Antarctic field experiments

develop electromagnetic methods of monitoring fluid transport and microstructural transitions

extensive measurements of fluid and electrical transport properties of sea ice:

2007	***Antarctic***	***SIPEX***
2010	***Antarctic***	***McMurdo Sound***
2011	***Arctic***	***Barrow AK***
2012	***Arctic***	***Barrow AK***
2012	***Antarctic***	***SIPEX II***
2013	***Arctic***	***Barrow AK***
2014	***Arctic***	***Chukchi Sea***

photo by Jan Lieser

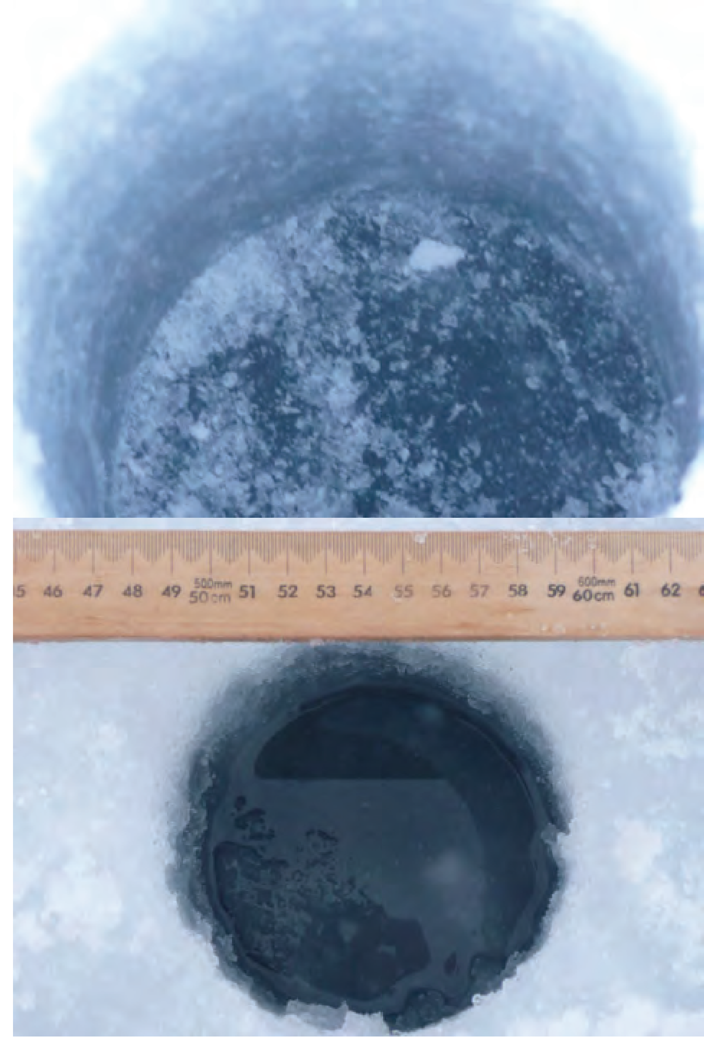

measuring fluid permeability of Antarctic sea ice

SIPEX 2007

higher threshold for fluid flow in Antarctic granular sea ice

columnar

granular

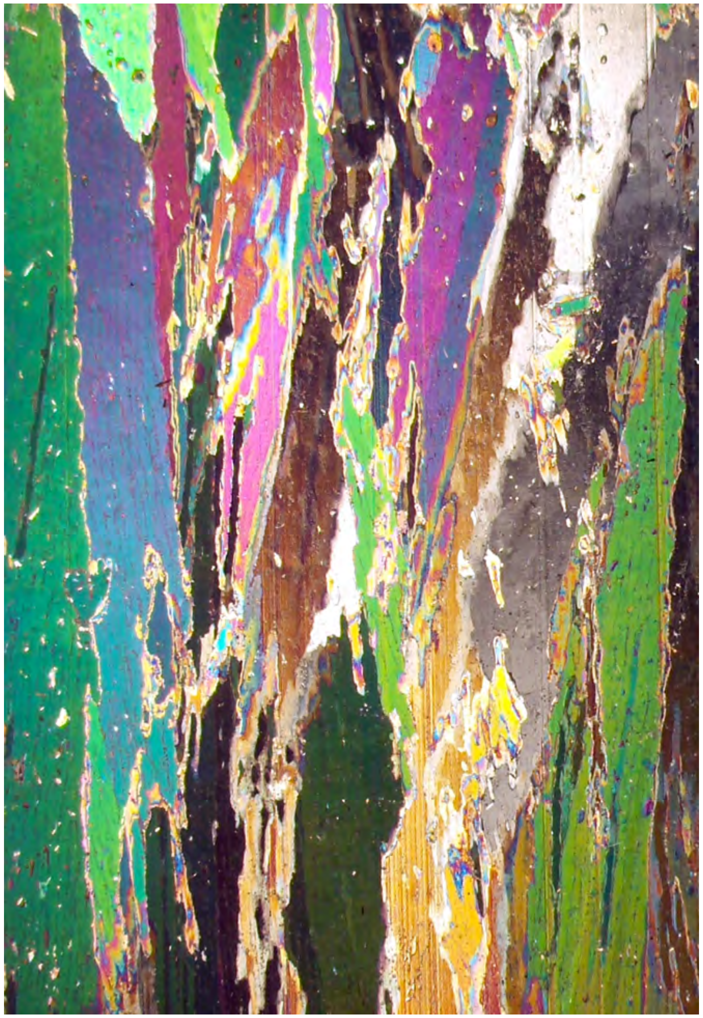

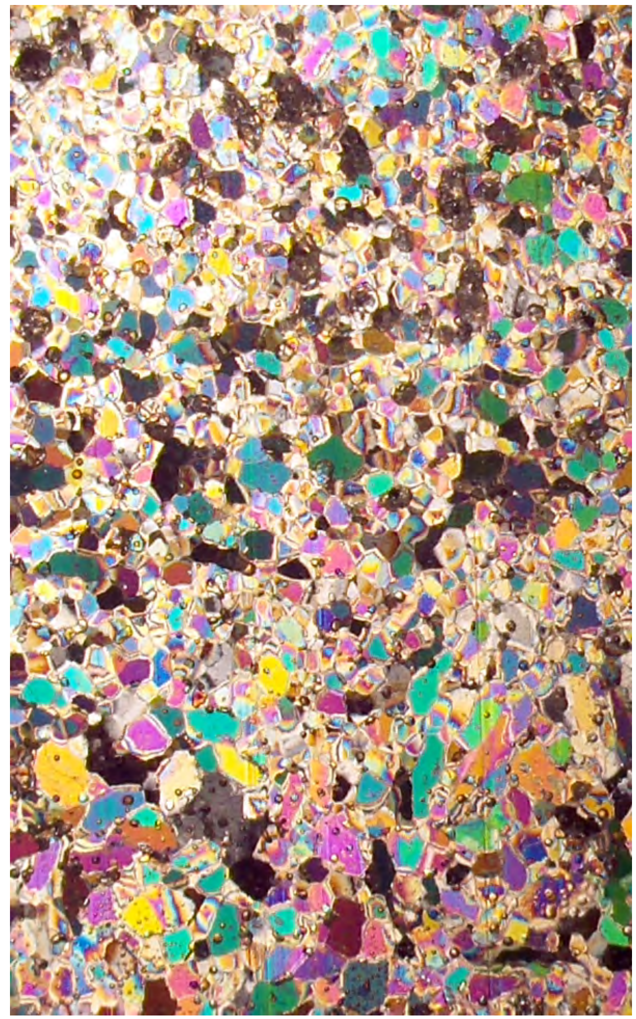

5%

10%

Golden, Sampson, Gully, Lubbers, Tison 2017

tracers flowing through inverted sea ice blocks

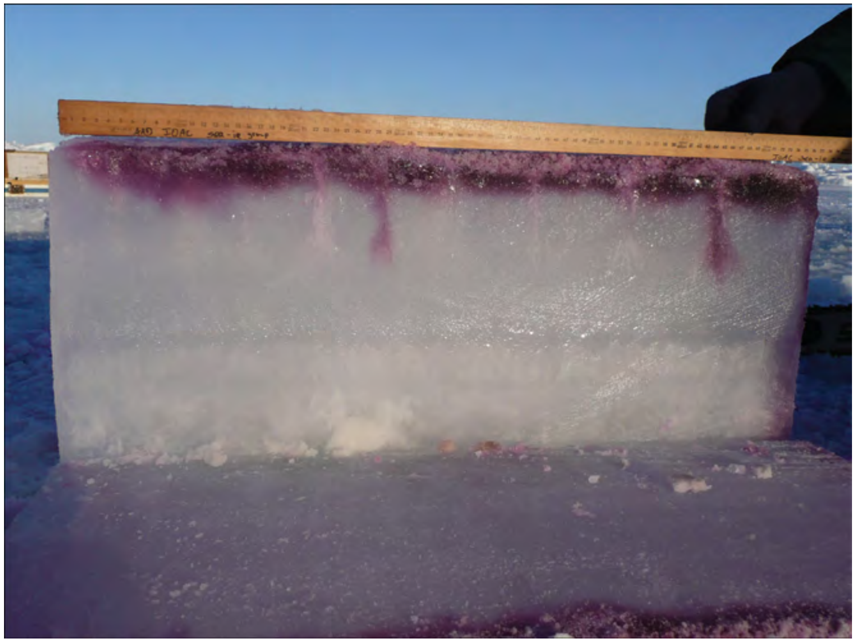

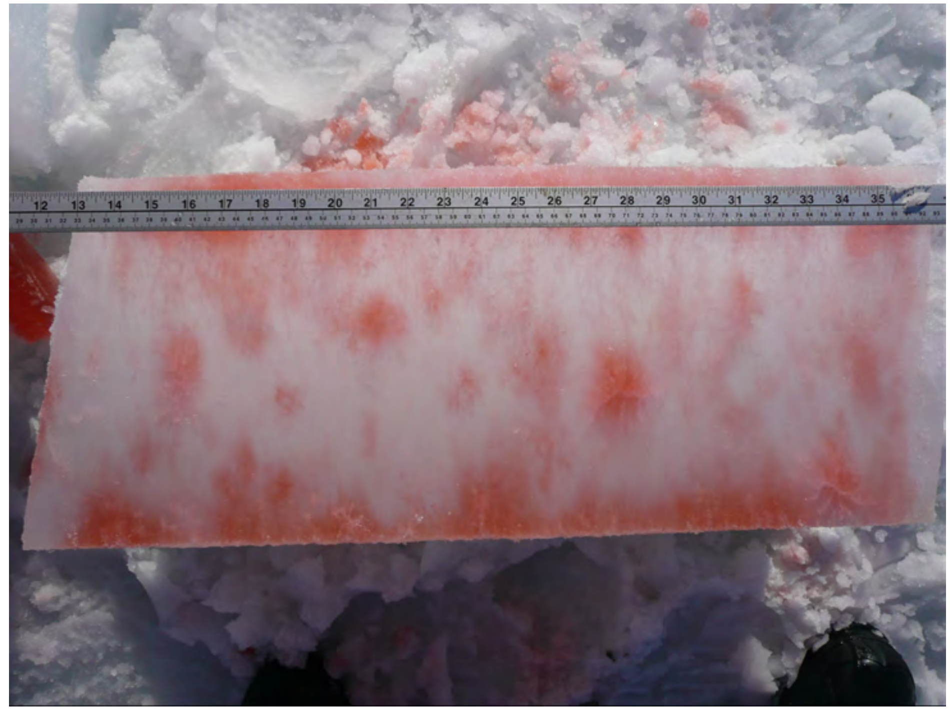

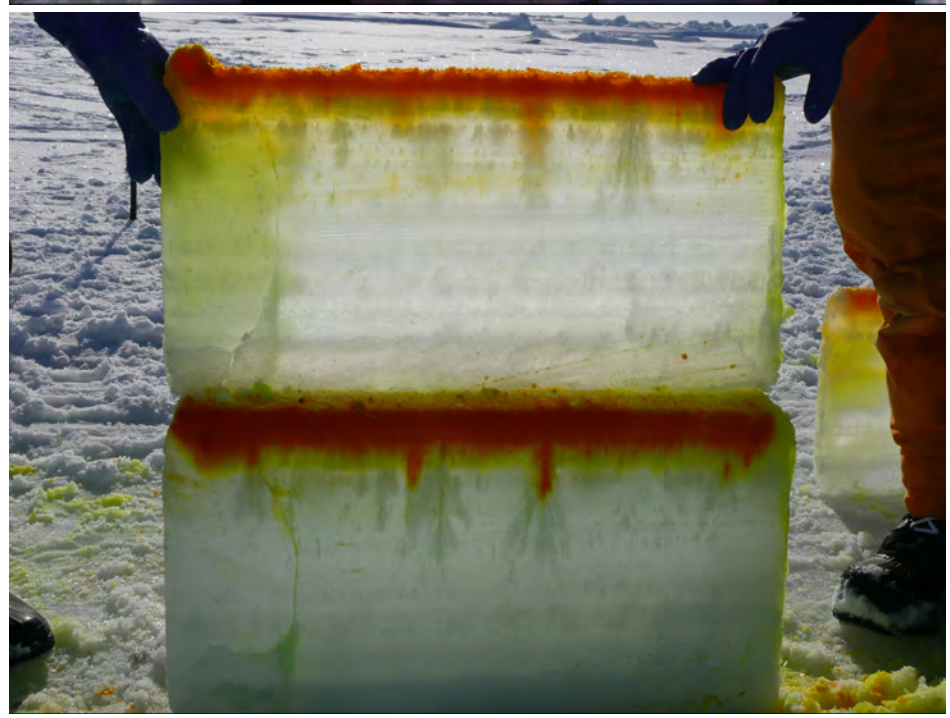

fractals and multiscale structure

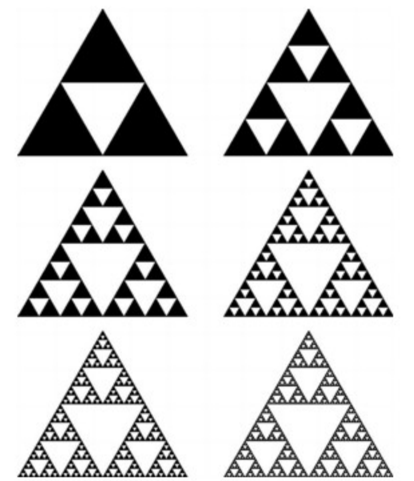

melt pond formation and albedo evolution:

- ***major drivers in polar climate***
- ***key challenge for global climate models***

numerical models of melt pond evolution, including topography, drainage (permeability), etc.

Lüthje, Feltham, Taylor, Worster 2006

Flocco, Feltham 2007

Skyllingstad, Paulson, Perovich 2009

Flocco, Feltham, Hunke 2012

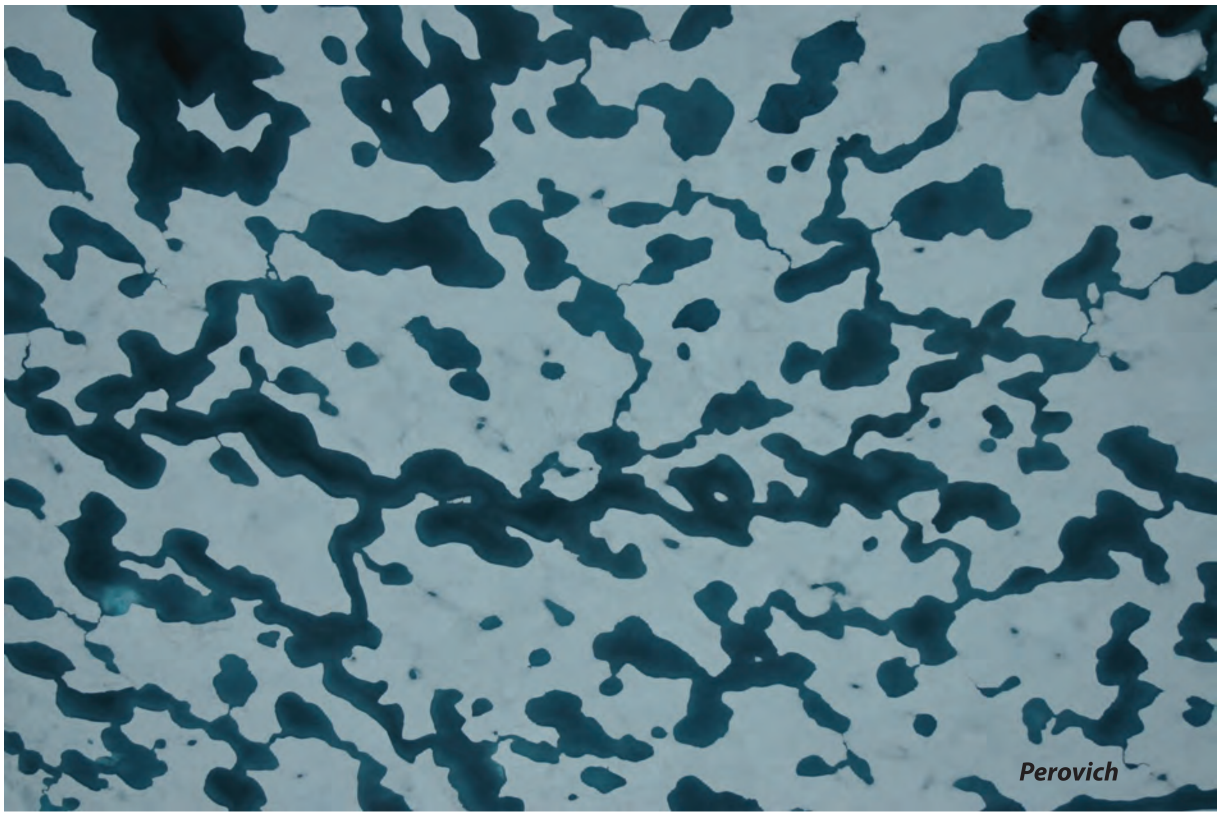

Are there universal features of the evolution similar to phase transitions in statistical physics?

Transition in the fractal geometry of Arctic melt ponds

The Cryosphere, 2012

Christel Hohenegger, Bacim Alali, Kyle Steffen, Don Perovich, Ken Golden

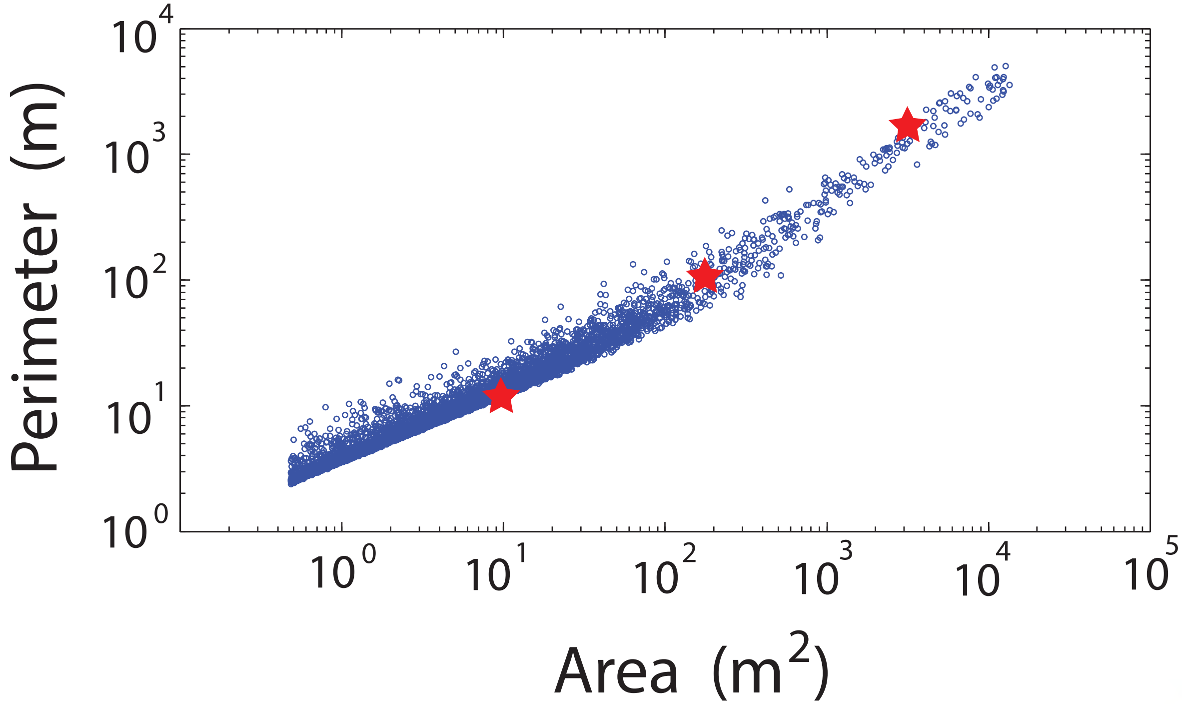

data from
5269 Arctic
melt ponds

simple pond ***transitional pond*** ***complex pond***

transition in the fractal dimension

complexity grows with length scale

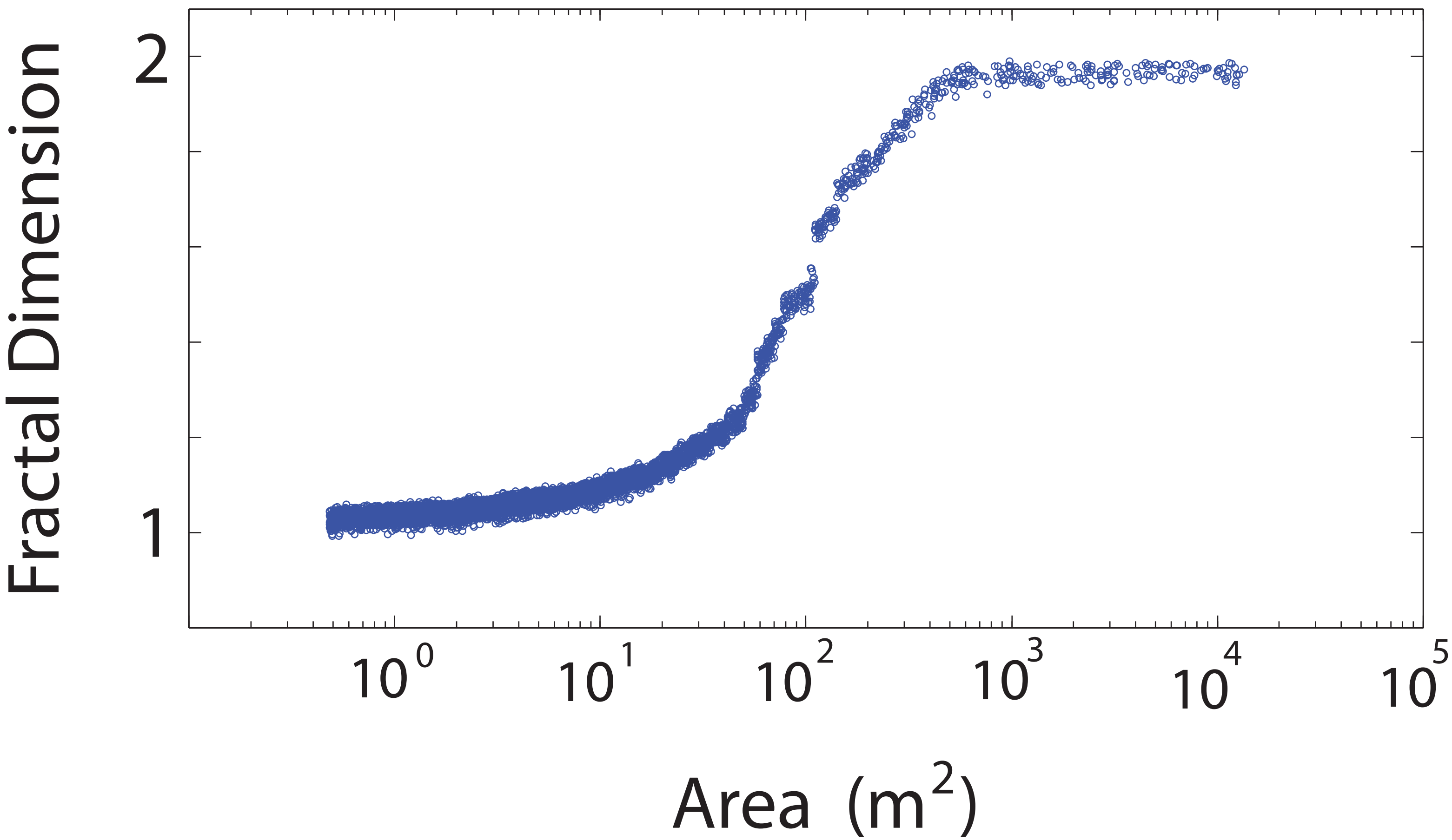

compute "derivative" of area - perimeter data

small simple ponds coalesce to form large connected structures with complex boundaries

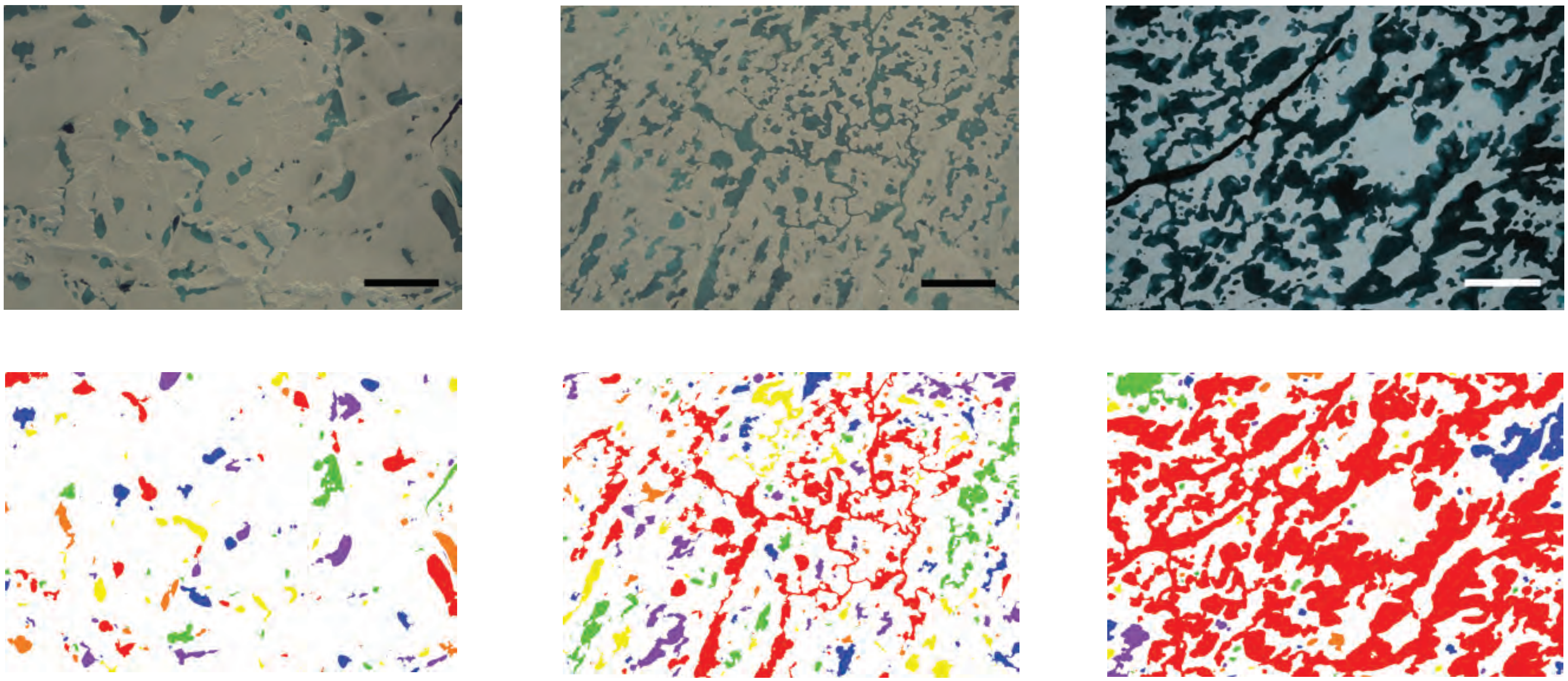

melt pond percolation

results on percolation threshold, correlation length, cluster behavior

Anthony Cheng (Hillcrest HS), Dylan Webb (Skyline HS), Court Strong, Ken Golden

Continuum percolation model for melt pond evolution

level sets of random surfaces

Brady Bowen, Court Strong, Ken Golden, J. Fractal Geometry 2017

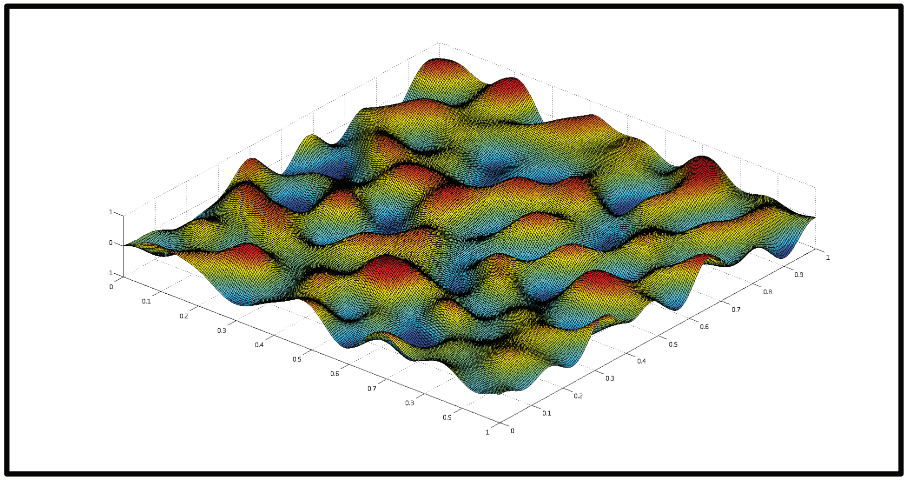

random Fourier series representation of surface topography

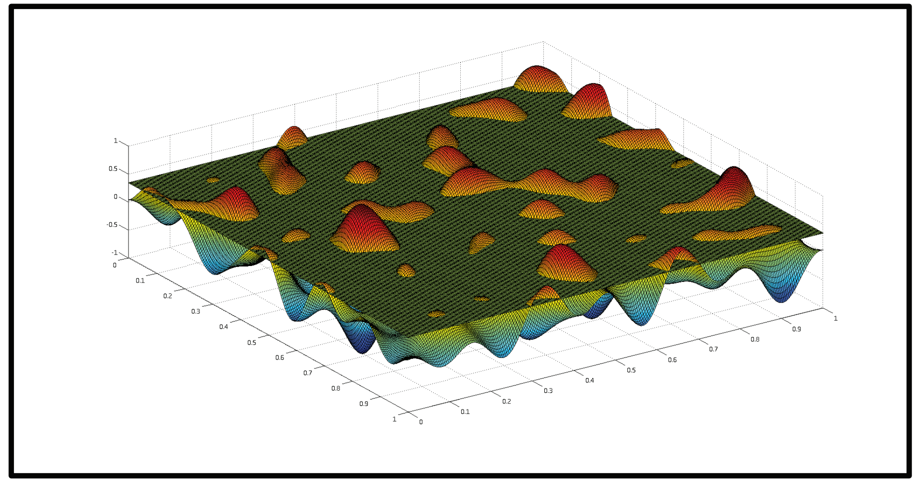

intersections of a plane with the surface define melt ponds

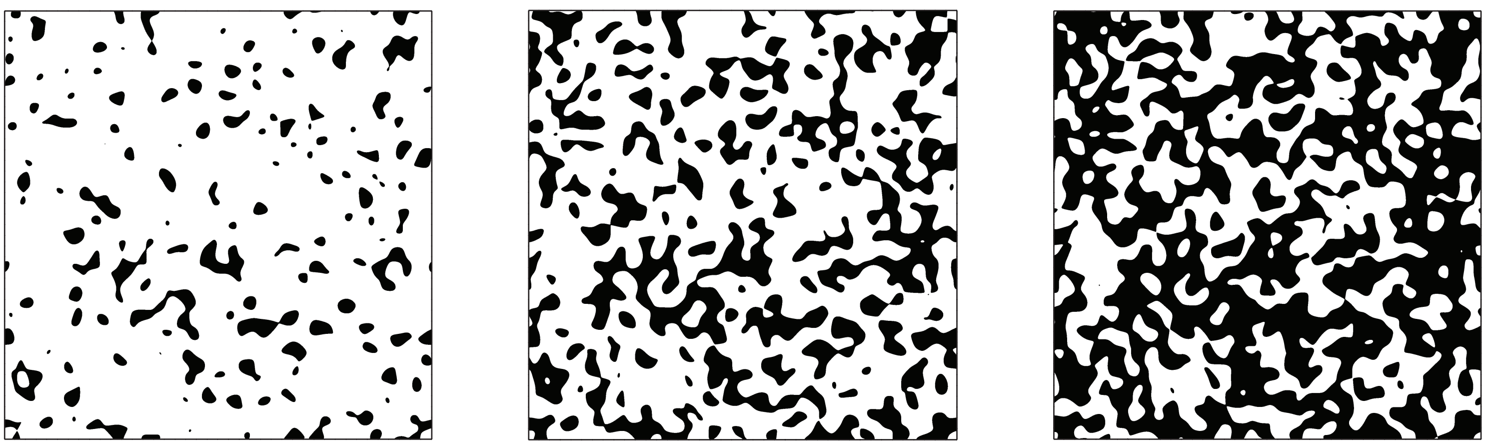

electronic transport in disordered media *diffusion in turbulent plasmas* *Isichenko, Rev. Mod. Phys., 1992*

melt pond evolution depends also on large-scale “pores” in ice cover

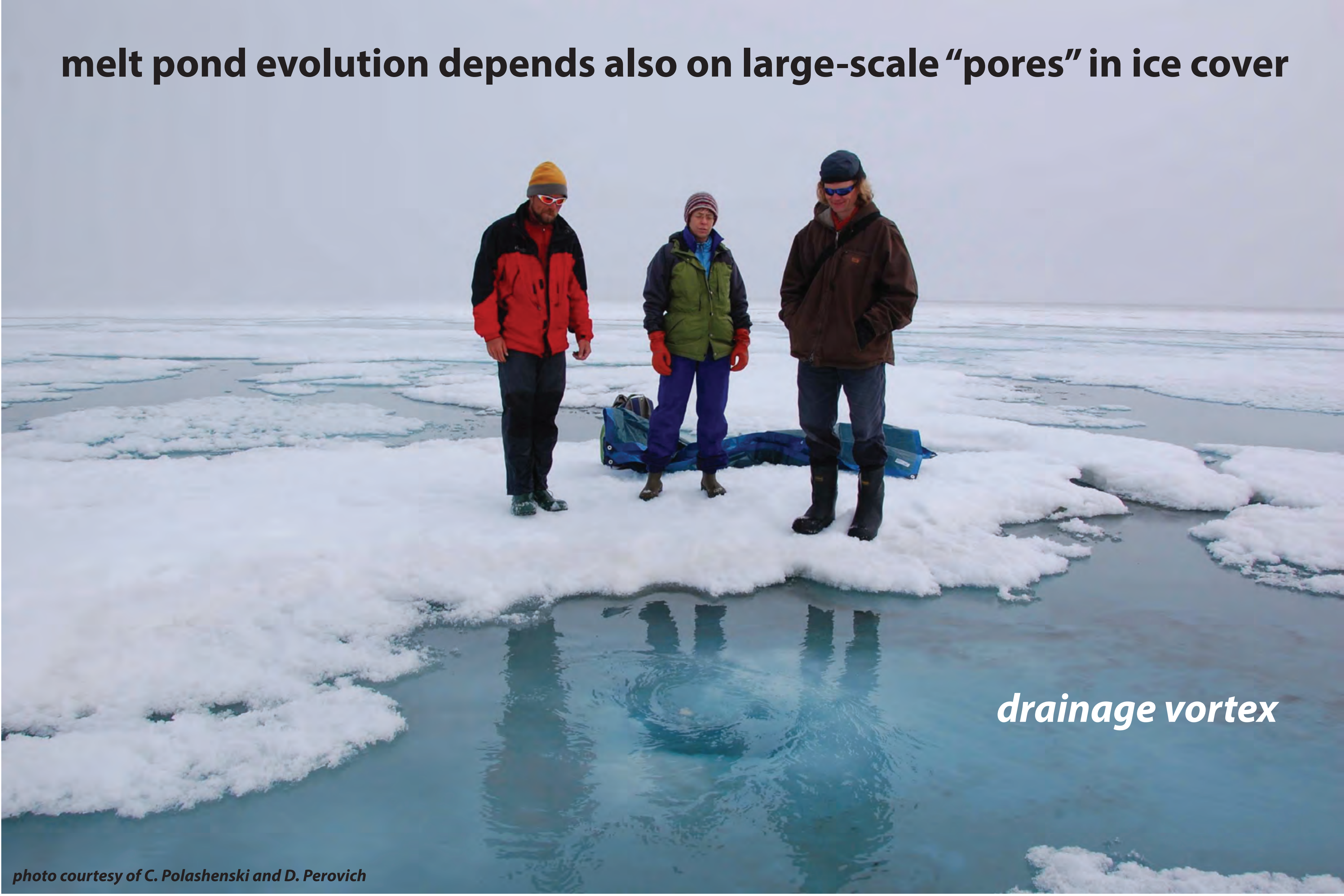

Melt pond connectivity enables vast expanses of melt water to drain down seal holes, thaw holes, and leads in the ice.

Network modeling of Arctic melt ponds

Barjatia, Tasdizen, Song, Sampson, Golden
Cold Regions Science and Tecnology, 2016

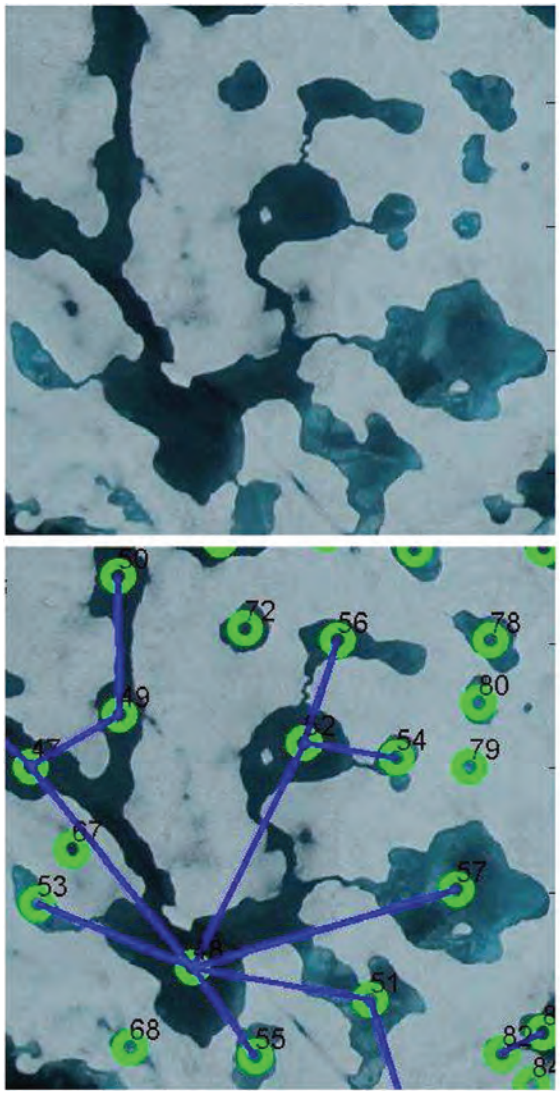

develop algorithms to map images of melt ponds onto

random resistor networks

graphs of nodes and edges with edge conductances

edge conductance ~ neck width

compute effective horizontal fluid conductivity

Ising model for ferromagnets → **Ising model for melt ponds**

$$\mathcal{H}_\omega = -J \sum_{<i,j>}^{N} s_i s_j - H \sum_i^N s_i \qquad s_i = \begin{cases} \uparrow & +1 \quad \text{water} \quad \text{(spin up)} \\ \downarrow & -1 \quad \text{ice} \quad \text{(spin down)} \end{cases}$$

magnetization $M = \lim_{N\to\infty} \frac{1}{N} \left\langle \sum_j s_j \right\rangle$ **pond coverage** $\frac{(M+1)}{2}$

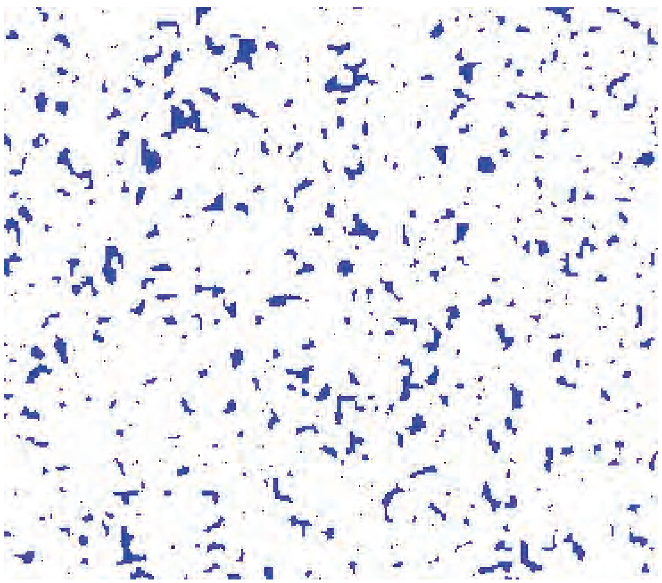

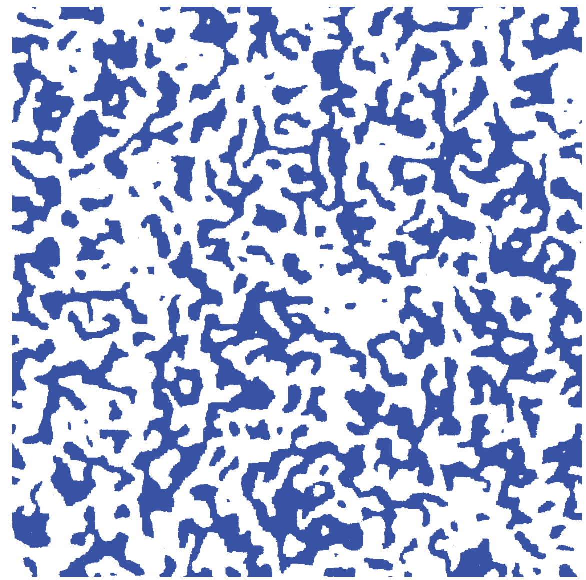

"melt ponds" are clusters of magnetic spins that align with the applied field

predictions of fractal transition, pond size exponent **Ma, Sudakov, Strong, Golden 2017**

The Melt Pond Conundrum:

How can ponds form on top of sea ice that is highly permeable?

C. Polashenski, K. M. Golden, D. K. Perovich, E. Skyllingstad, A. Arnsten, C. Stwertka, N. Wright

Percolation Blockage: A Process that Enables Melt Pond Formation on First Year Arctic Sea Ice

J. Geophys. Res. Oceans 2017

2014 Study of Under Ice Blooms in the Chuckchi Ecosystem (SUBICE) aboard USCGC Healy

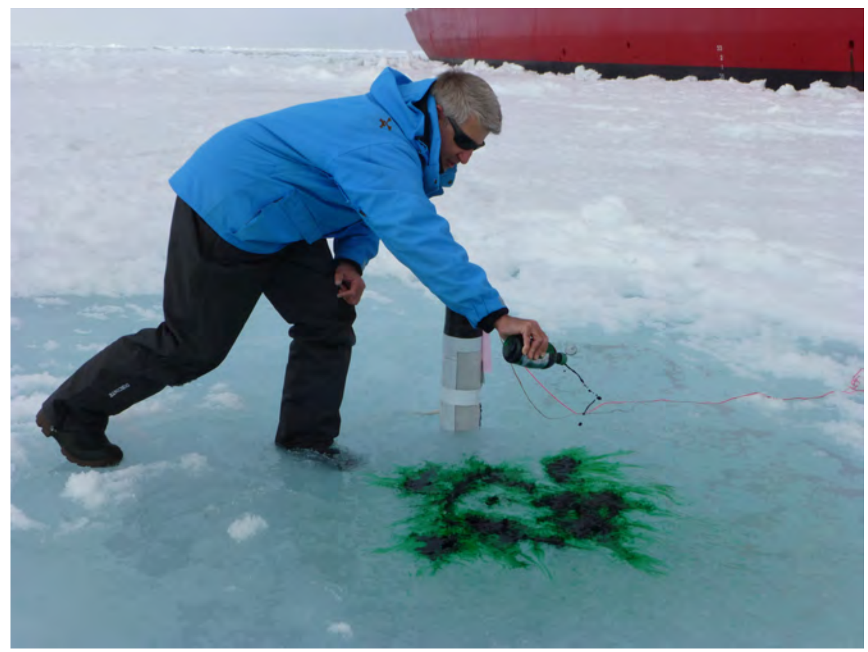

Conclusions

1. Summer Arctic sea ice is melting rapidly, and melt ponds and other processes must be accounted for in order to predict melting rates.

2. Fluid flow through sea ice mediates melt pond evolution and many processes important to climate change and polar ecosystems.

3. Homogenization and statistical physics help *link scales*, provide rigorous methods for finding effective behavior, and advance how sea ice is represented in climate models.

4. Critical behavior (in many forms) is inherent in the climate system.

5. Field experiments are essential to developing relevant mathematics.

6. Our research will help to improve projections of climate change, the fate of Earth's sea ice packs, and the ecosystems they support.

THANK YOU

National Science Foundation

Division of Mathematical Sciences

Division of Polar Programs

Office of Naval Research

Arctic and Global Prediction Program

Applied and Computational Analysis Program

Mathematics and Climate Research Network

Australian Government
Department of the Environment and Water Resources
Australian Antarctic Division

ANTARCTIC CLIMATE & ECOSYSTEMS
COOPERATIVE RESEARCH CENTRE

Antarctica New Zealand

UNIVERSITY OF ALASKA FAIRBANKS

THE UNIVERSITY OF UTAH

Buchanan Bay, Antarctica   Mertz Glacier Polynya Experiment   July 1999